Ph.D DISSERTATION

A STUDY ON BODY COMMUNICATION ANTENNAS

인체통신용 안테나에 관한 연구

BY
SUMIN YUN

FEBRUARY 2015

SCHOOL OF ELECTRUCAL ENGINEERING
AND COMPUTER SCIENCE
COLLEGE OF ENGINEERING
SEOUL NATIONAL UNIVERSITY

공학박사 학위논문

A STUDY ON BODY COMMUNICATION ANTENNAS

인체통신용 안테나에 관한 연구

2015년 2월

서울대학교 대학원

전기·컴퓨터 공학부

윤 수 민

Abstract

This thesis presents the antennas for in-body, on-body communication. The antennas in body communication are severely affected by human body which has a high relative permittivity and conductivity. The high relative permittivity and conductivity degrades the antenna bandwidth and efficiency. Therefore, it is a main challenge that enhancing the bandwidth and the efficiency of the antenna maintaining the small size. In order to enhance the performance of the antennas several techniques are proposed in body communication antennas.

Firstly, the Q value and the efficiency of the in-body antenna are investigated. Using the proposed equations, the optimum frequency of the in-body antenna will be given. To maximize the antenna dimensions in the endoscopy antenna, the outer wall loop antennas is proposed. The measurement results are given to show the performance of the proposed antenna.

Secondly, the several techniques for on-body antenna are proposed. The conventional antennas without the ground plane like dipole and slot antennas are not appropriate for on-body environment because the body has low intrinsic impedance and high conductivity compared to that of the free space. Therefore, antennas with ground plane like patch and cavity-backed slot antennas are proposed for on-body communication. The cavity-backed slot antenna with via-hole above the slot is

proposed for bandwidth enhancement of the antenna. As the place of the via-hole introduces the additional resonance, wider bandwidth is achieved. The substrate removal technique for cavity-backed slot antenna is also proposed for the bandwidth and the efficiency enhancement. The removal of the substrate across the slot decreases the Q of the antenna, increasing the bandwidth and efficiency. In addition, the folded-cavity-backed slot antenna is given for size miniaturization of the cavity-backed slot antenna. The folded structure of the proposed antenna increases the effective length of the antenna, decreasing the antenna resonance frequency. Furthermore, the reconfigurable shorted patch antenna is given for wide bandwidth. Lastly, the dual-band and dual-impedance cavity-backed slot antennas are given for the efficient on-body systems

Keywords: capsule endoscopy antenna, outer-wall antenna, cavity-backed slot antenna, patch antenna, reconfigurable antenna, wide-band antenna, high efficient antenna, miniaturization, dual-band, dual-impedance.

Student number: 2008-22942

Contents

List of Figures

List of Tables

Chapter 1

Introduction

1.1 Wireless Body Area Network (WBAN)

As the life expectance is increasing with advance of medicine, population aging is unavoidable worldwide trend. The advances of the diagnosis techniques, like MRI (Magnetic Resonance Imaging), ultrasonography, CT (Computed Tomography), endoscopy enable the detection of small tumors, which are invisible to the naked eye.

For the health examination, the patient should be at hospital to utilize the diagnosis facilities. It usually takes much time to checkup the body. This time consuming process may prevent the patient from regular checkup, especially for the elderly. Therefore, needs for easy and comfortable diagnosis technique is increasing.

With a help of wireless communications, traditional diagnosis methods are expected to be changed. The various diagnosis techniques have been proposed using

WBAN (Wireless Body Area Network). The WBAN is a network of wearable and embedded computing devices. The advances of low power integrated circuits, physiological sensors, small antenna and battery have miniaturized the whole system enough to be attached or embedded to a human body. The WBAN allows cost effective and continuous health monitoring using the physiological sensors. The gathered medical records are monitored with real-time through the wireless communication [1]–[4].

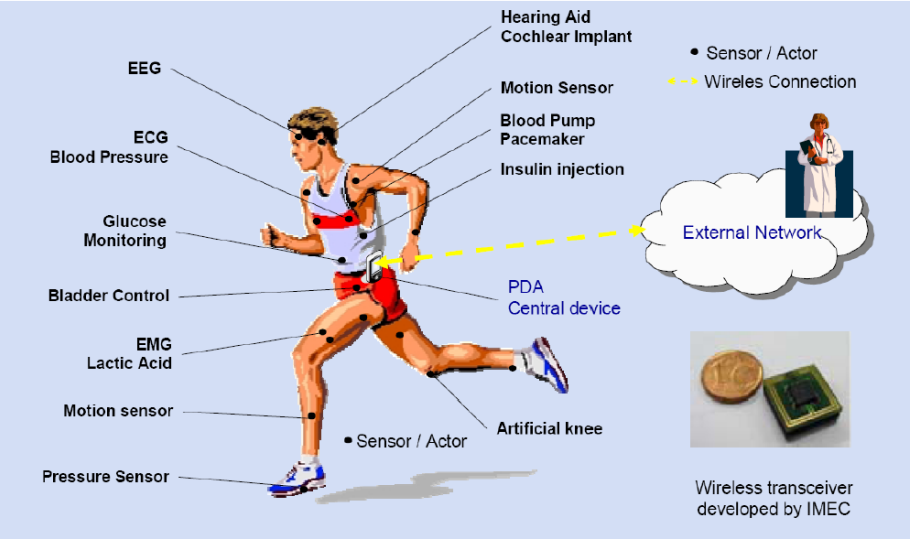

Fig. 1.1 Wireless Body Area Network [2].

One of the famous applications using WBAN is capsule endoscopy. In the traditional endoscopy, the endoscope should be inserted to the digestive tracks for

the monitoring of the human body. Because this process is usually accompanied with pain and nausea, many traditional endoscopy are performed under local anesthetics. The use of capsule endoscopy can decrease the pain and nausea dramatically. As the capsule endoscopy moved along the human digestive systems, the camera captures the image of the digestive system. The captured image is transmitted to the external receiver outside the human body. The patient can have a social life instead of lying on the bed. The doctor investigates the gathered image for the monitoring after the whole procedure is over [5]–[7].

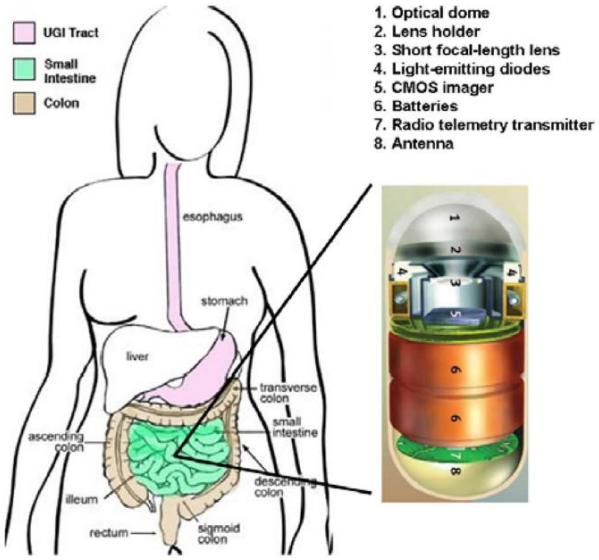

Fig. 1.2 Complete digestive track and the typical components found within an endoscopy capsule system [7].

There are also many implant devices using WBAN techniques. The pace maker

can be integrated with a transmitter for the monitoring of a heart rate and remaining battery capacity [8]–[10]. The stent which is inserted to a blood vessel also can be integrated with a transmitter [11], [12] for the monitoring of a blood pressure and flow.

The intensive researches are also conducted on the on body WBAN. The various sensors are suggested for the monitoring of the vital signs. The gathered data is transmitted to off-body receiver or wearable devices. The long time monitored data can be used for the diagnosis. Also the sudden changes of the vital signs can alert the hospital directly even before having a heart attack or stroke. The WBAN is a promising technology for the future medical services.

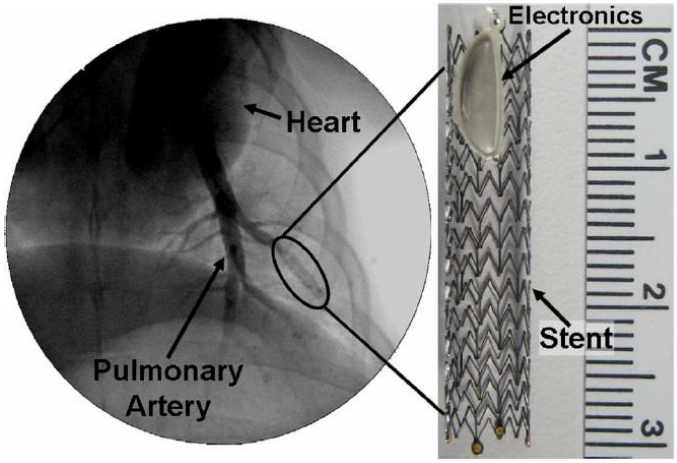

Fig. 1.3 Implanted stent with a transmitter [12].

Several frequency bandwidths are allocated for the WBAN services. The MICS (Medical Implant Communication Service) is allocated from 402 MHz to 405 MHz for the implant services. The FCC has approved the allocation 40 MHz, from 2360 MHz to 2400 MHz, for the medical low-power BAN links. WBAN services also can utilize the Wi-Fi bands for the data transmission.

The most challenging issue in designing WBAN systems is a low efficiency problem. As the transmitting power of the embedded and wearable devices are limited by SAR (Specific Absorption Rate) regulations and battery capacity, the system efficiency is especially important in WBAN systems. However, the electric properties of the human body significantly decrease the bandwidth and the efficiency of the antenna. Efficient and wide band antenna is essential in designing the high efficient WBAN systems.

1.2 Electric Properties of Human Body

The antennas in body communication systems are partially or totally enclosed by the human body. Therefore, the electric properties of the human body have a significant effect on operation of the body communication antenna. The electric properties of the human body should be considered in designing body communication antennas.

A human body is composed of various organ and tissues. Different tissues have

different electric properties. Furthermore, electric properties of same tissues can be slightly changed according to the weight, age, race, life styles. In this thesis, the dielectric properties of a human body from FCC are used for human model. For example, the electric properties of a human body at 2400 MHz can be obtained from FCC [13] as shown in TABLE 1.1.

Table 1.1 : Electric properties of a human tissue at 2.4 GHz

Tissue	ε_r	σ (S/m)
Bladder	18.02	0.67
Blood	58.34	2.50
Colon(Large_Intestine)	53.96	1.99
Fat	5.28	0.10
Heart	54.91	2.21
Kidney	52.85	2.39
Liver	43.11	1.65
Lung(Inflated)	20.50	0.79
Muscle(Parallel_Fiber)	54.49	1.84
Skin(Dry)	38.06	1.44
Small_Intestine	54.52	3.13
Thyroid_Thymus	57.27	1.92
Tongue	52.69	1.76

It is hard to consider the whole body tissues in designing a body communication antenna because of the available computational processing speed. Therefore, the body is modeled as a homogeneous material in designing the in body antenna. Also the body is modeled as a homogeneous or 3-layer model in designing on body antennas. The simplification of a human model enables time efficient body communication antenna design.

1.3 Challenges in Designing Body Communication Antenna

The electric properties of a human body are considerably different from the substrates used in RF systems as shown in Table 1.1. The muscle has a relative permittivity of 54.49 and a conductivity of 1.84 S/m at 2.4 GHz. The high relative permittivity and conductivity cause narrow bandwidth and low efficiency problems.

The resonance frequency and radiation resistance of the dipole antenna in free space can be approximately calculated by

$$f_0 \approx \frac{c}{2l}, \quad R_0 = 73\,\Omega \quad \text{in free space} \tag{1.1}$$

where the c and l are the light velocity and the length of the dipole. When the dipole is surrounded by an infinite media, the resonance frequency and the radiation resistance of dipole changes to

$$f_r \approx \frac{f_0}{\sqrt{\varepsilon_r \mu_r}} , \qquad R_r \approx \sqrt{\frac{\mu_r}{\varepsilon_r}} R_0 \tag{1.2}$$

where ε_r and μ_r are the relative permittivity and the relative permeability of the infinite media. The radiation resistance decreases as the relative permittivity increases. This is called dielectric loading effect. The matching circuits used for impedance matching may cause narrow bandwidth problems. Also, the miniaturized size of the antenna by a dielectric material causes narrow band problems. Although the antenna miniaturization by dielectric loading effect is desirable, overcoming of the narrow bandwidth is also required in body communication antenna design.

The high conductivity of a human body causes serious antenna efficiency problems. In the free space environment, the radiated power or reactive energy does not attenuated. However, in body area network environment, considerable reactive energy and radiated power dissipate by dielectric losses in a human body. The dielectric losses around the antenna reduce the antenna efficiency. The dielectric loss inside a human body also increases the SAR of a human body. Fig. 1.4 shows that SAR simulation of a dipole antenna when dipole is placed on a human chest. To meet the SAR limitation with high antenna efficiency, the techniques for reducing dielectric loss around antenna are required.

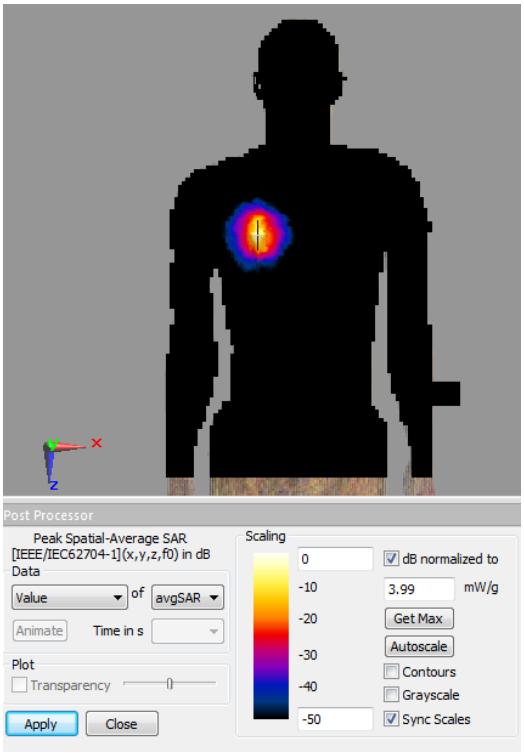

Fig. 1.4 SAR of the dipole antenna on human chest.

In this thesis, several techniques for high antenna efficiency, wide band, and antenna miniaturization are proposed for the body communication antennas. The operation principles and simulated and measured results are presented. The effect of the proposed antenna will be discussed in this thesis.

Chapter 2

Antennas in Human Body

2.1 Properties of the Antenna in Human Body

The antennas for implant medical devices and the endoscopy system are surrounded by the human body. Therefore, it is helpful to review the properties of the antenna surrounded by a lossy medium. It is well known that the bandwidth, gain, and the efficiency of the antenna depend on the size of the free space antenna [14]. Therefore, the antenna performances are limited by the size of the antenna [15]. Antennas inside a lossy medium are also affected by the size of the antenna [16], [17].

For the BAN antenna design, the quality factor (Q) and the radiation efficiency of the spherical modes inside the human body will be investigated in this chapter. The Q and a radiation efficiency of the spherical modes inside a given size of

antenna can be used as a guideline for designing in body communication antennas.

2.1.1 Radiation Efficiency of the Antenna in Human Body

The antenna efficiency is a crucial factor evaluating the performance of the antenna. As the antenna efficiency is directly multiplied in calculation of the system efficiency, designing a highly efficient antenna is essential in BAN applications. The Fig. 2.1 shows the reflected and the radiated power of the antenna. The antenna efficiency, η_a , is defined as

$$\eta_a = \frac{P_r}{P_i} = \eta_r (1 - |\Gamma|)^2 \tag{2.1}$$

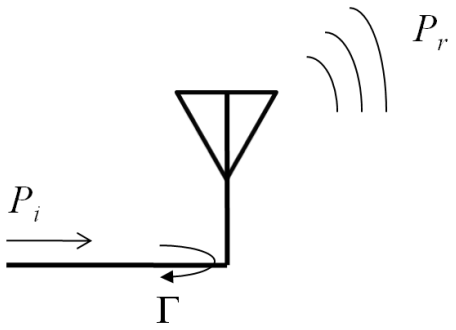

Fig. 2.1. Radiated and reflected power of the antenna.

where P_r is the radiated power, P_i is the total input power, η_r is the radiation efficiency, Γ is the reflection coefficient of the antenna. In most systems, the

requirement for antenna return loss is higher than 10 dB. It means that the returned power from the antenna input is usually less than 10 % of the input power. Therefore the antenna efficiency, which is directly proportional to the radiation efficiency, is the main factor determining the antenna efficiency of the antenna.

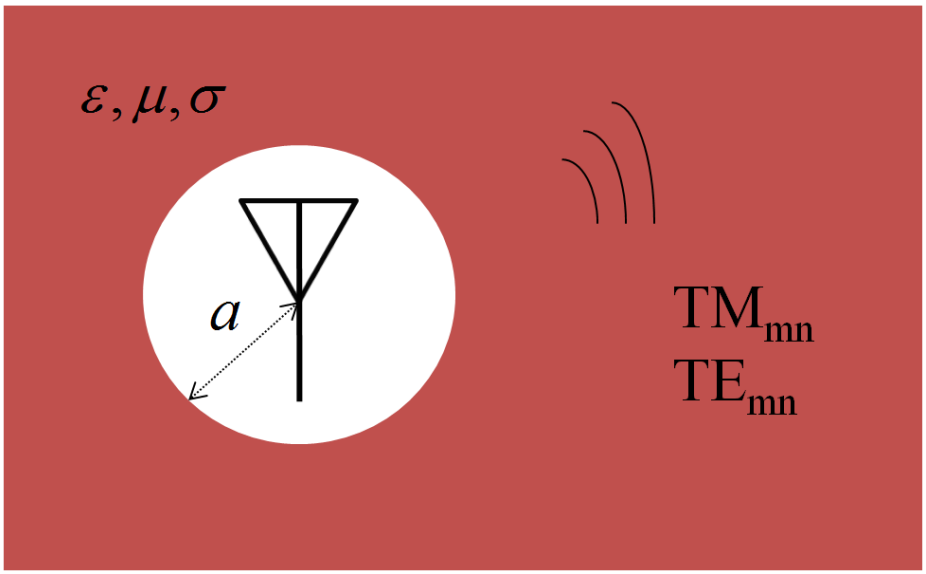

Fig. 2.2. Antennas in a lossy medium.

The radiation efficiency depends on the current distribution of the antenna. An antenna and a feeding structure determine the current distribution of the antenna. In many applications like satellite, military, mobile communications, the antenna dimensions are usually larger than body communications antennas. Thus, there is freedom in modifying the structure of the antenna for the favorable current distribution. For the case of the body communication antenna, the current

distribution is quietly limited compared to the other applications.

The antennas which have dimensions shorter than 1/10 wavelength is called as small antenna. As the majority in body antennas have a small dimensions compared to the wavelength of their resonance frequency, the in-body antennas can be classified as small antennas. The small antennas usually generate fundamental spherical modes in operation. Therefore, the radiation efficiency of the fundamental spherical modes determines the radiation efficiency of the in body communication antenna.

The complex power from the antenna at a distance r, $S(r)$, can be described as

$$S(r) = P_r + P_d + j2\omega(W_m - W_e) \tag{2.2}$$

Where the ω, W_m, W_e are the angular velocity, the stored magnetic energy, the stored electric energy, respectively. Then, the radiated power of the antenna can be expressed as in [16]

$$\begin{aligned} P_r(r) &= \mathrm{Re}\{S(r)\} \\ &= P_r(a)e^{-2|\mathrm{Im}(k)|(r-a)} \\ &= \eta_r \,\mathrm{Re}\{S(r)\}e^{-2|\mathrm{Im}(k)|r} \end{aligned} \tag{2.3}$$

$$where \quad \eta_{\mathrm{r}} = \frac{P_r(a)}{\mathrm{Re}\{S(r)\}} e^{2|\mathrm{Im}(k)|a} \tag{2.4}$$

Then the radiation efficiency is given as [16]

$$\eta_r = \begin{cases} \dfrac{\mathrm{Re}\{\eta\}}{\mathrm{Re}\left\{ j\eta \hat{H}_n'(ka)\hat{H}_n(ka)^* \right\}} & \text{TM mode} \\ \dfrac{\mathrm{Re}\{\eta\}}{\mathrm{Re}\left\{ -j\eta \hat{H}_n(ka)\hat{H}_n'^*(ka) \right\}} & \text{TE mode} \end{cases} \tag{2.5}$$

Where η is an intrinsic impedance of the medium, k is the wave number of the medium.

2.1.2 Q of the Antenna in Human Body

The quality factor or Q of resonator is strongly connected to the bandwidth of the resonator. The Q of the resonator is defined as

$$Q = 2\pi \frac{\text{Time-average energy stored at a resonant frequency}}{\text{Energy dissipated in one period of this frequency}} \tag{2.6}$$

The Q factor is a measure of the bandwidth of the resonator. The investigation of the Q factor in a lossy medium gives an insight on design of the in body antennas. The Q of the spherical modes in a lossy medium can be calculated using following equations [17]

$$\begin{aligned} Q_{TM} &= (1-\eta_{r.TM} e^{-2|\mathrm{Im}(k)|a}) \cot\delta \\ Q_{TE} &= \eta_{r.TE} (\frac{1}{\eta_{r.TM}} - e^{-2|\mathrm{Im}(k)|a}) \csc\delta \end{aligned} \tag{2.7}$$

Where δ=tan ($\varepsilon_i/\varepsilon_r$)

2.1.3 Numerical examples and conclusion

The Q and the radiation efficiency of the fundamental spherical modes are calculated in the homogeneous human body model. The human body is modeled as a homogeneous material which has an electric properties, ε_r = 58, σ = 0.85 S/m. The calculation was conducted at 500 MHz, where the transmission loss was optimum when a = 5 mm, R = 15 cm, G_{RX} = 1, as shown in Fig. 2.3 [18].

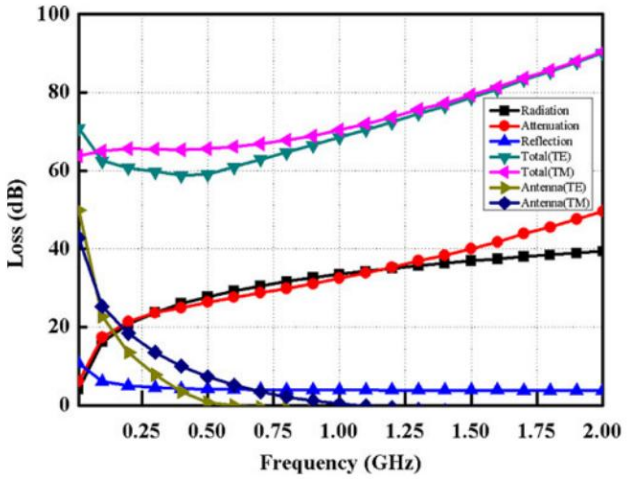

Fig. 2.3 Transmission Loss through the human body [18].

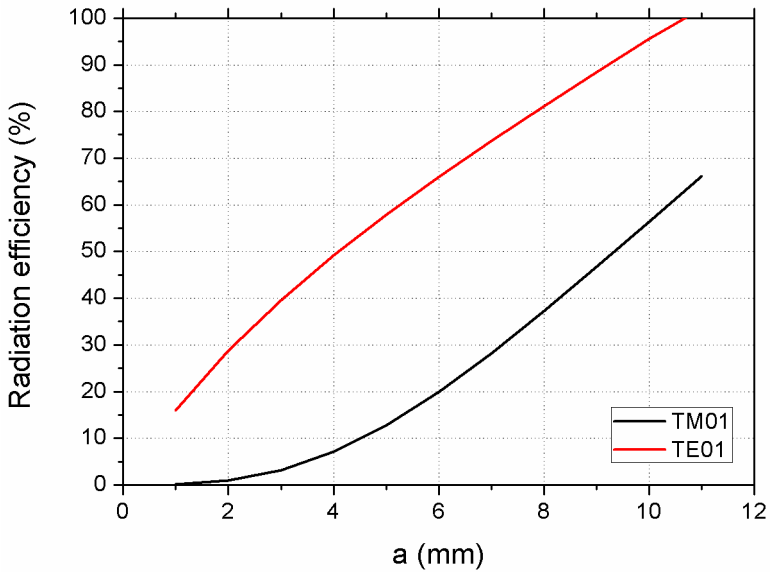

Fig. 2.4 Radiation efficiencies of TE_{01} and TE_{01} spherical modes

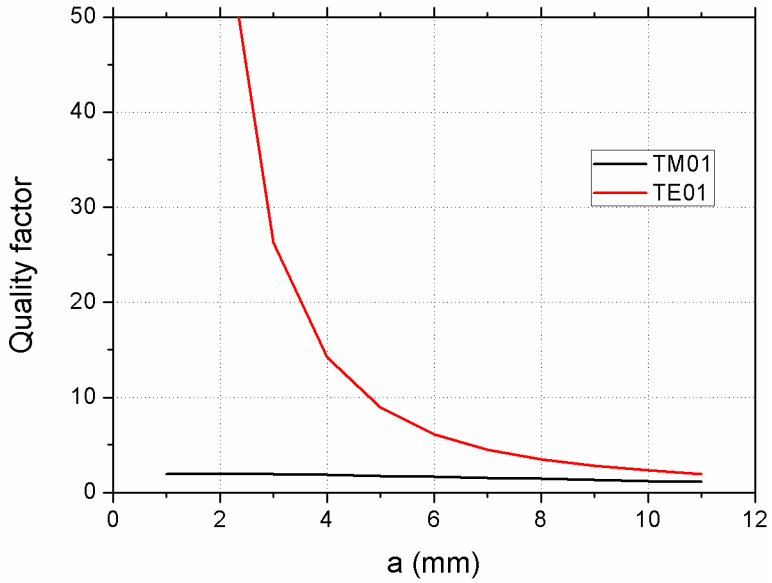

Fig. 2.5 Quality factors of TE_{01} and TE_{01} spherical modes.

Fig. 2.4 and Fig 2.5 show the radiation efficiency and the quality factors of TE_{01} and TE_{01} modes, respectively. From this graphs, it is obvious that as the antenna size increases, the efficiency and the bandwidth can be increased. Therefore, having the large dimensions of the antenna is highly favorable. However, the size of the in body antenna is usually limited to the certain size. The antenna should fully utilize the given size limit to have a wide bandwidth and a high efficiency.

2.2 Outer-Wall Loop Antenna for Capsule Endoscope System

Capsule endoscopy system has been used to obtain an image from the inside of the human digestive tract. To acquire high resolution images, a loop antenna with ultra wide bandwidth is proposed. It is part of the outer wall of the capsule, thus decreasing volume and increasing performance, and uses a meandered line for resonance in an electrically small area. The proposed antenna makes maximal use of the capsule's outer surface, enabling the antenna to be larger than inner antennas. The measured result shows that the gain of proposed antenna is higher than that of inner antennas. Return loss and radiation pattern are investigated through simulation and measurement, showing that the proposed antenna has an ultra wide bandwidth of 260 MHz (from 370 to 630 MHz) for VSWR < 2, and an omni-directional radiation pattern. Using identical antenna pairs in the equivalent body phantom fluid, antenna efficiency is measured to 43.7 % (-3.6 dB).

2.2.1 Introduction

The capsule endoscopy system uses a wireless transceiver system to obtain medical images of the inside of the human body [19]. This wireless inspection has changed the way subjects are examined. A subject just takes the endoscopy capsule and lives a normal life. The swallowed capsule travels through the digestive tract,

gathering images from the camera module and transferring them to the external receiver, where they are saved. Medical diagnosis can made after inspection of these images. This wireless alternative also creates less discomfort when compared to conventionally intrusive methods.

Transmit power in a capsule endoscope system is limited by the safety guide for human body to EM field and by the battery capacity. Also, the data rate is limited by the bandwidth of the system. An Ultra Wide Bandwidth (UWB) capsule endoscope system using Chirp Spread Spectrum Modulation was proposed to obtain higher data rate than 10 Mbps with low power consumption [20].

As the capsule moves through the digestive tract, properties of the body tissue surrounding it change. Therefore, narrow band antenna can be detuned due to the various material properties. A UWB antenna, however, could maintain its operation because of its ultra wide band characteristic. UWB also enables monitoring through high resolution images. However, designing a UWB antenna into the capsule is fundamentally difficult due to the fact that the capsule size is electrically small.

For wideband operation, monopole antennas enclosed by capsule were presented [21], [22] with wide bandwidth around 500 MHz. Their cylindrical volume, however, occupies space inside the capsule, which increases the size of the capsule and makes it uncomfortable to swallow.

To decrease the minimum size of the capsule, dipole antenna with meandered

line was fabricated on the outer wall of the capsule [23]. It had a higher center frequency (1.4 GHz) than monopole antennas [21], [22]. Lines of dipole are meandered in the way current is aligned for the extension of effective length of the antenna. It enveloped only the top dome of the capsule, and achieved polarization diversity by a meandered dipole line. However, its bandwidth was less than 200 MHz, not wide enough for a UWB system at 1.4 GHz.

In this section, we propose a UWB antenna fabricated on outer wall of the capsule. In small antenna theory, as the radius of sphere including the full antenna structure increases, the limitation of radiation efficiency increases [15]. Since the proposed antenna uses the whole capsule surface, it is expected to show better radiation efficiency than antennas inside the capsule. The proposed antenna therefore not only saves capsule volume, but also increases radiation efficiency.

2.2.2 Antenna Design

During the entire endoscopy procedure, the capsule is surrounded by lossy body tissues that significantly reduce the signal strength and affect the radiation of the antenna. Therefore, it is essential to investigate propagation in a lossy medium.

To investigate these effect, the human body is considered as an averaged homogeneous medium as described by Federal Communication Commission (FCC) [13]. The homogeneous human body model is shown in Fig. 2.6. The permittivity

and conductivity of the body change with the change in operating frequency.

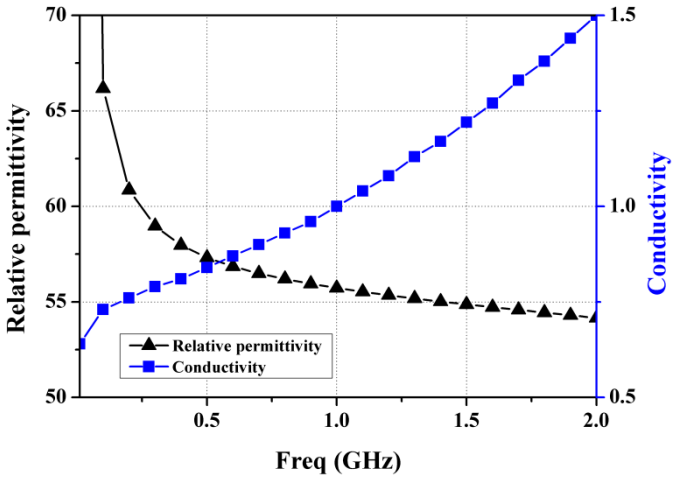

Fig. 2.6. The homogeneous human body model [24].

On the basis of the Friis's formula, the total loss between transmitter and receiver was calculated with the distance between the transmitting and the receiving antennas set to 15cm. It was calculated that the minimum total loss is achieved when operation frequency is between 400~600 MHz [24]. So the operation frequency of the proposed antenna is determined around 500 MHz.

As the size of the antenna is limited by the properties of the capsule, the dimensions and material properties of the capsule should be described first. The capsule is made of the dielectric material ultem (relative permittivity 3.15) which is very stable against variation of temperature, humidity, and frequency. The outer and

the inner radius of the capsule are 5.5 mm and 5 mm respectively. Its length is 24 mm. The top dome lies over the camera, so it is excluded from the design area as antennas there could affect image quality. The conductor used for antenna structure is copper. Gold or other stable materials can also be used for safe operation.

The fundamental design issue in designing capsule antenna is the antenna miniaturization, as at 500 MHz, the free space wavelength (60 cm) is much larger than the capsule length. Fortunately, the homogeneous body material surrounding the capsule has high permittivity, giving a dielectric loading effect [25] which significantly reduces the effective wavelength. Thus, it is relatively easy to design a small antenna in the human body than in air.

The proposed antenna is placed on the outer wall of the capsule, as illustrated in Fig. 2.7 It is a full wavelength loop antenna with symmetric pattern with respect to center of the capsule. The resonance frequency depends on the length of the loop. For resonance in the electrically small design area, the loop length needs to be extended. A meander technique is suitable for this purpose. By meandering sides of the loop antenna, total length can be increased enough to resonate at 500 MHz. The height of the meander line and the gap between meander patterns can be used as tuning parameters. After adjusting the dimension of the meander and number of meander patterns, the optimum values of these parameters are obtained. The height

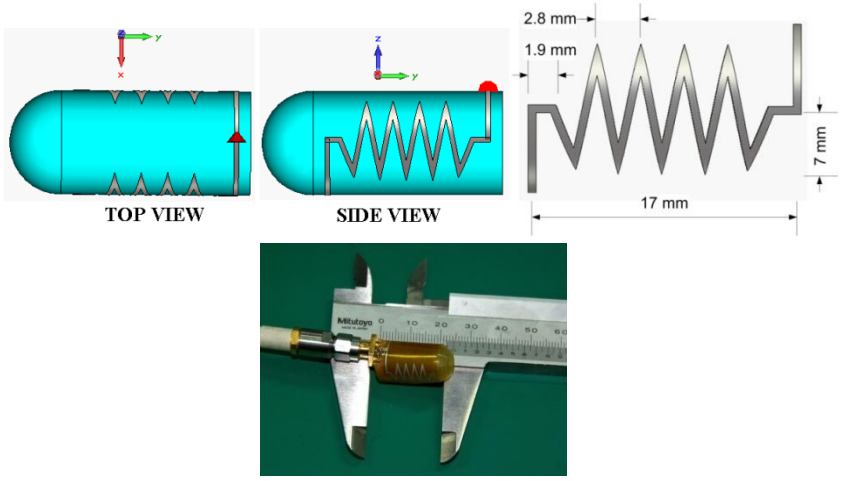

Fig. 2.7 Proposed outer wall loop antenna.

of the meander line and gap between meander patterns are set to 7 mm and 2.8 mm respectively. The opposite side of the loop line is meandered in the same way. The feeding point of the proposed antenna is indicated by a triangle in Fig. 2.7

2.2.3 Simulation and Measurement

In simulation, the external medium of the capsule is set to homogeneous body equal material (relative permittivity 56.4, conductivity σ = 0.82 S/m at 500 MHz) referring to FCC [13]. The antenna is placed at the center of body equal material. The simulation is performed using CST Microwave Studio.

The proposed antenna is fabricated on a flexible PCB with a polymide of thickness 25.4 μm and a copper line of thickness 18 μm. The fabricated antenna is attached to the outer wall of capsule as illustrated in Fig. 2.7. For differential feeding,

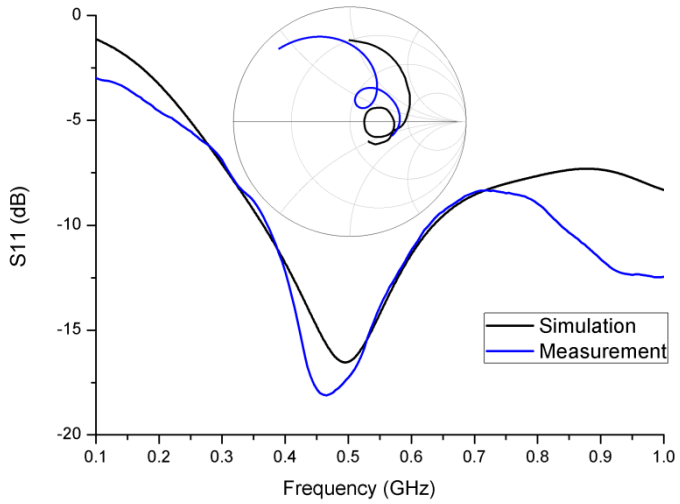

Fig. 2.8. Simulated and measured reflection coefficient

BALUN (Analen B0322J5050A00) is used at the feeding point of the antenna, with a SMA connector connected to the unbalanced line of the balun. For measurement, the capsule is inserted in the plastic container filled with human equivalent phantom with the same electrical characteristics as averaged homogeneous body at 500 MHz.

The simulated return loss and the measured return loss in human equivalent phantom are presented in Fig. 2.8. The measured result shows that the proposed antenna has an ultra wide bandwidth ranging from 370 MHz to 630 MHz for VSWR < 2. The measured result agrees well with the simulated result. With 50 % fractional bandwidth, proposed antenna can be used in UWB system.

The endoscopy capsule should contain many electrical components, i.e., camera, battery, PCB. However, electrical components near antenna can affect its operation

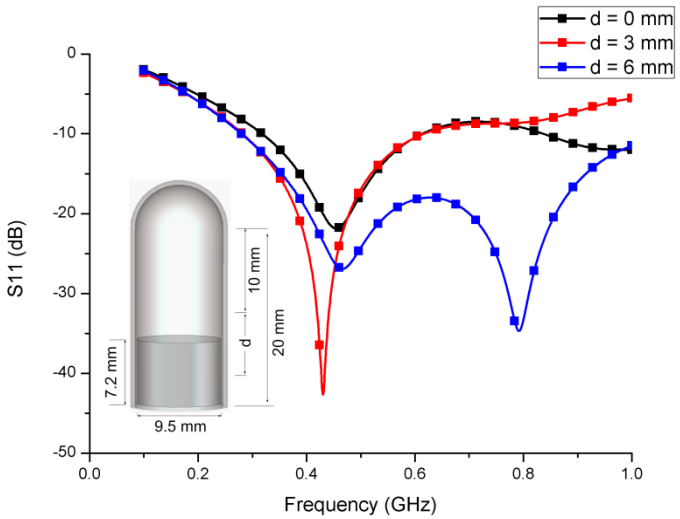

Fig. 2.9. Simulated return loss with battery in various position. (d: distance from the center of cylindrical capsule face to the center of the battery)

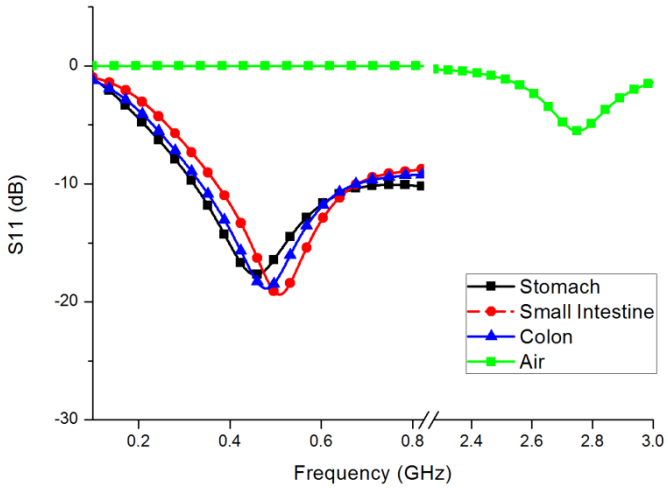

Fig. 2.10 Simulated return loss in various tissues.

of the outer wall loop antenna. Because of their size, batteries are expected to have the most significant effect. Batteries are simply represented as a PEC cylinder with diameter 9.5 mm and height 7.2 mm as shown in Fig. 2.9. By adjusting distance from the center, effects of batteries in various positions are simulated.

The simulated return losses are shown in Fig. 2.9. Although there are decreases in resonance frequency, return losses lower than -10 dB is maintained around 500 MHz.

Once a capsule is swallowed, it passes stomach (ε_r = 66.706, σ = 1.035 S/m), small intestine (ε_r = 63.876, σ = 1.958 S/m), colon (ε_r = 66.706, σ = 1.035 S/m, all at 500 MHz) and other small digestive organs. Fig. 2.10 shows the simulated return loss of the proposed antenna in various tissues and air. Because of its UWB characteristic, it can maintain S11 lower than -10 dB for a range of ±100 MHz about the center frequency. In air, first resonance of the proposed antenna occurs at 2.75 GHz and the radiation efficiency at first resonance is simulated to -0.025 dB.

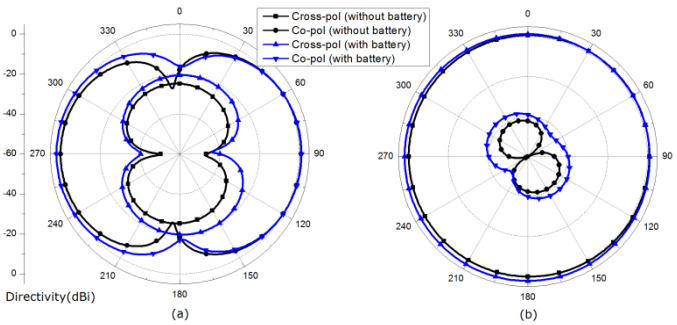

Fig. 2.11 Simulated radiation patterns of the proposed antenna. (a) in xy-cut plane (b) in yz-cut plane.

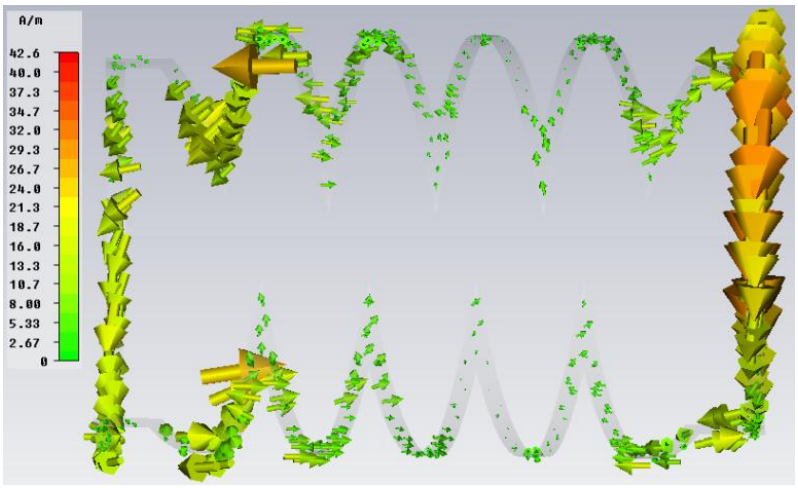

Fig. 2.12 Current distribution along the antenna structure.

The radiation pattern of the proposed antenna is shown in Fig. 2.11. It indicates that the proposed antenna pattern is omni-directional like a conventional dipole antenna. The radiation pattern considering battery is also simulated with battery is placed at d = 6 mm. It has a similar pattern with that of the battery free case except slight increase in the directivity.

To illustrate its operation, current distribution is presented in Fig. 2.12. Current is oriented downward at the feeding point which is placed at one end of the loop. It flows to the opposite end of the loop. Since current changes its direction at the center of the meander pattern, maximum current flows in same direction at the each end of the antenna.

TABLE 2.1

AVERAGED MEASURED POWER

Antenna	Normalized power (dB)	Dimension (mm)
Outer Wall Loop	-1.37	11 x 11 x 17
Monopole Spiral	-4.71	10.1 x 10.1 x 3
Fat Monopole Spiral	-5.62	10 x 10 x 4

Two aligned currents make radiation pattern similar to the dipole pattern. At the center of the meander pattern, radiations from meander pattern are out of phase to each other, because the current is reversed at the center of the meander pattern. As currents in the meander line cancel out, they contribute little to radiation.

Compared with antennas inside the capsule, outer wall antennas use the given design space maximally. In small antenna theory, as antenna size increases,

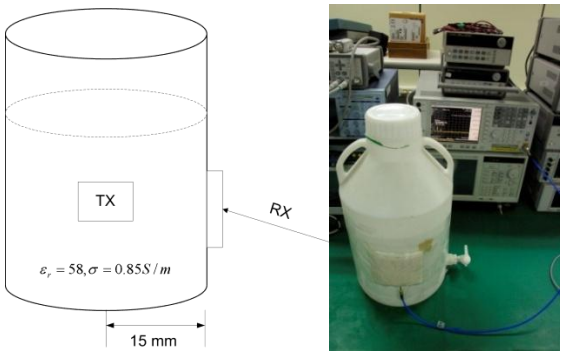

Fig. 2.13 Measurement setup.

limitation of maximum gain increases. Therefore, it is expected that an outer wall antenna would have a higher gain than an inner antenna. We compared the gain of the proposed antenna with those of inner antennas in the same capsule at 500 MHz. Fat monopole spiral antenna [21] and monopole spiral antenna [22] are used as reference inner antennas. Dimensions of each antenna are shown in Table 2.1. They have wide VSWR < 2 bandwidth either side of 500 MHz. Inner monopole antennas and the proposed antenna have omni-directional radiation patterns at 500 MHz. We compared gain in the H-plane, using measurement setup illustrated in Fig. 2.13 The antenna to be measured is placed at the center of a plastic container filled with human equivalent phantom. Each antenna is integrated with the same transmitter of which output power is 1 mW [26]. The receiving antenna is placed outside of the container, 15 cm from the transmitter. Received power is measured using a power spectrum and normalized to the maximum value of the received power when transmitter is integrated with the outer wall loop antenna. The result is shown in Fig. 2.14 and Table 2.1.

The result shows that, in overall angle in H-plane, the outer wall antenna has higher gain than inner antennas. As we expected, the receiving antenna on the surface of the container could receive more power when power is transmitted by the outer wall loop antenna.

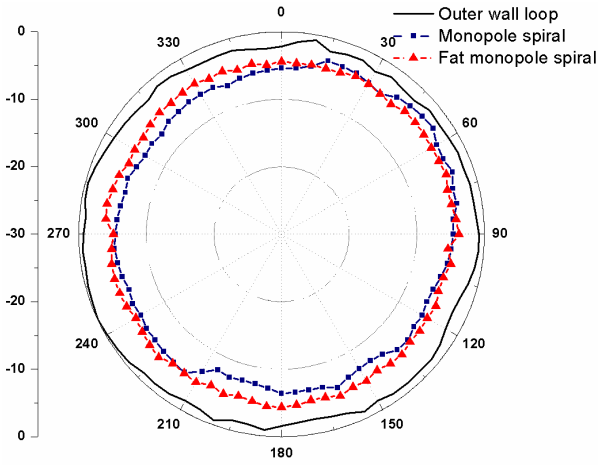

Fig. 2.14 Normalized measured power of receiving antenna.

Using an identical outer wall loop antenna in the human equivalent phantom, antenna efficiency is calculated. One antenna is set to transmitter and the other to receiver, with the H-planes of each antenna in the same plane. Then we can measure receiving power from a transmitter with 1 mW. The distance between two antennas set to 15 cm. Because the effect wavelength in human equivalent phantom at 500 MHz is 7.633 cm, 15 cm is enough for satisfying the far field conditions.

From the received power, antenna efficiency can be calculated from Friis's formula. Attenuation loss in the human equivalent phantom and insertion loss of balun is also considered in the calculation. The simulated directivity of 1.9 is used in calculation as illustrated in Fig. 2.11.

In measurement, received power is -57.8 dBm. Using Friis's formula, antenna efficiency of the proposed antenna is calculated to be 43.7 % (-3.6 dB).

2.2.4 Conclusion

A loop antenna with meander pattern is proposed for a UWB endoscope system. It is fabricated on the outer surface of the capsule, thus reducing the size of the capsule by the volume previously occupied by the inner antenna. Although capsule size is reduced, the radius of sphere enclosing the entire structure of antenna is increased, giving higher gain than an inner antenna. The proposed antenna has omni-directional radiation patterns, favorable in endoscopy communication.

The proposed antenna has VSWR < 2, a bandwidth of 260 MHz (from 370 MHz to 630 MHz), and radiation efficiency of 43.7%. With its UWB characteristics and high radiation efficiency, it can be used in UWB endoscope systems.

In this work, the TM mode (dipole mode) is utilized for the antenna operation. However, as illustrated in Fig. 2.4, the TE mode (loop mode) has a higher radiation efficiency compared to that of the dipole mode. The radiation efficiency can be further enhanced by generating TE mode. For the generation of the loop mode, the antenna structure having a uniform loop current should be designed. Overcoming the low radiation efficiency of the small loop antenna maintaining the uniform current will be a main issue in designing TE mode capsule endoscopy antenna.

Chapter 3

Antennas on Human Body

3.1 Properties of the antenna on Human Body

In many BAN applications, antennas are placed on the human body. Depending on the applications, antennas are placed on a wrist, chest, neck, ankle, etc. As the body tissues behind the on body antenna also have considerably high relative permittivity and conductivity, the on body antennas are also severely affected by the body. In the following sections, the performances of the several antennas are simulated on the human body. The simulated data is used for selecting the fundamental antenna in design on body antennas.

3.1.1 Modeling of the Human Body

The tissue composition can be substantially different according to the location

of the human body. Also the physical condition and age and gender also cause differences in tissue composition. Therefore, the standard modeling for the human body is required for the design of the on body antennas.

For the simplification of the human body, three body tissues are included in the modeling as shown in Fig. 3.1. At the top of the on body model, the skin layer is included. The muscle layer is placed bottom of the model. Between the skin and the muscle layer, subcutaneous adipose tissues which have varying amounts of fat are included. The thickness and electric properties at 2.4 GHz of the each layer are found in [13], [27]–[29]. In the following on body antenna design, 3 - layer model or homogeneous model are used for simulation.

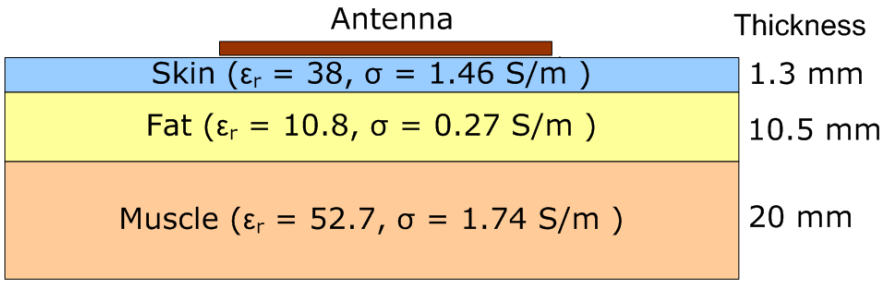

Fig. 3.1. 3-layer on body model

3.1.2 Antennas without Ground on Human Body

The first step of antenna design may be a decision on the fundamental structure of the antenna. The selected fundamental antenna will be modified to the certain type of the antenna to meet the requirement for the antenna performance. The proper selection of the fundamental antenna can decrease the design time significantly.

In this sections, antenna without ground plane are simulated on the body model to give a guideline in selection of the fundamental antenna. The simulation was conducted as shown in Fig. 3.2. The human body is modeled as homogeneous material which has the electric properties of ε_r=35.15, σ=1.16 S/m. The dimensions of the human body are 100 x 100 x 50 mm^3. The conventional half wavelength dipole antenna and the slot antenna placed on the 1 mm height RT 5880 substrate are simulated. The radiation efficiencies of the each type of antennas are obtained with a different distance between antennas and the body model as shown in Fig. 3.3.

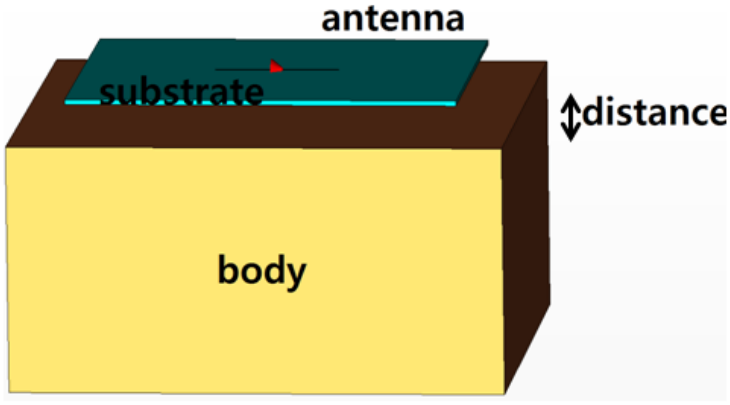

Fig. 3.2. The simulated on-body environment

Fig. 3.3 shows that the radiation efficiency of the antenna decreases as the distance between antenna and a body model decreases at 2.4 GHz. As the most on body antennas are placed very closed to the body, it is quiet difficult to design high efficient on body dipole antenna. When the distance is less than 1 mm, that radiation efficiency is lower than 10 %. Compared to the radiation efficiencies in the free space, which are higher than 90 %, the radiation efficiencies are very poor. As the intrinsic impedance of the body is lower than that of the free space, most radiated power was dissipated inside the human body. In [30], it was reported that the dipole antennas attached directly to the human body has radiation efficiency less than 1 %. From these results, we can conclude that the conventional antennas without the ground plane are not suitable for on body antennas.

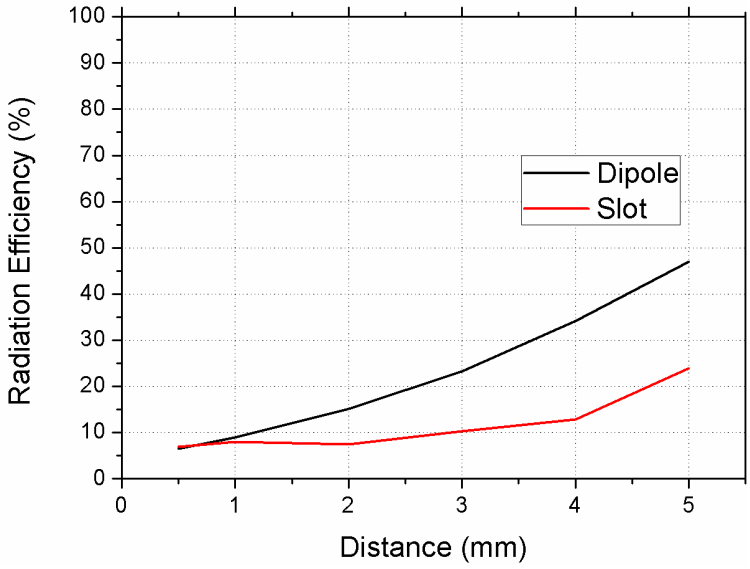

Fig. 3.3. Radiation efficiency of the dipole and slot antenna on human body

3.1.3 Antennas with ground plane on body

There are many types of antenna which have a ground plane themselves. A cavity-backed slot antenna and a patch antenna is a typical antenna which have a ground plane. We simulated these antennas on the body model same way used in antennas without ground plane. Fig. 3.4 shows the radiation efficiency of two antennas. The radiation efficiency also decreases as the distance between antenna and the body decreases. However, the amount of decrease was much smaller than that of the antenna without ground plane. When the distance was 0.5 mm, both antennas have radiation efficiency higher than 80 %. Because the ground plane between the body and the radiating element eliminates the effect of the body, high radiation efficiency is obtained.

There are some drawbacks of the antennas with ground plane. Main problem is a size and a bandwidth. A narrow bandwidth of a patch and a cavity-backed slot antenna may not be appropriate in some applications.

Furthermore, compared to a dipole and a slot antennas which are the basically line antennas, the cavity-backed slot antenna and a patch antenna occupy the area. These drawbacks can limit the wide use of a patch and a cavity-backed slot antenna.

In the following sections, several techniques are proposed to overcome the bandwidth and size problems. Also some techniques for enhancing the radiation efficiency will be proposed.

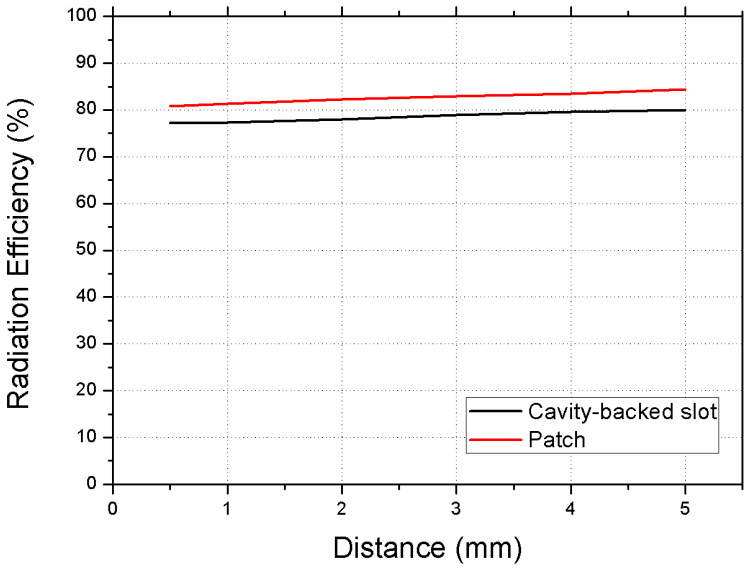

Fig. 3.4. The radiation efficiency of a cavity-backed slot and patch antenna.

3.2.1 Operation of Cavity-backed Slot Antenna

The conventional slot antenna has a bidirectional radiation pattern. Its bidirectional radiation pattern is not suitable for on body applications because the antenna is significantly affected by the medium behind the antenna.

For the suppression of the back side radiation of the conventional slot antenna, the cavity-backed slot antenna was proposed. A cavity-backed slot antenna is composed of a slot and a quarter guided wavelength cavity. Because the quarter guided wavelength cavity makes parallel resonance, which has high impedance around the resonance frequency, the back side radiation can be suppressed effectively. Fig. 3.5 shows the radiation patterns of the slot and the cavity-backed slot antennas. The conventional slot antenna illustrated in Fig. 3.5 has a bidirectional radiation patterns, which is not suitable for on body antennas. For the case of the cavity-backed slot antenna, the radiation to the backside of the antenna is significantly decreased by placing the quarter wavelength cavity behind the antenna. As the quarter-wavelength cavity under the slot may not be suitable in many applications, the cavity is usually bent into the parallel direction as shown in Fig. 3.6 [31].

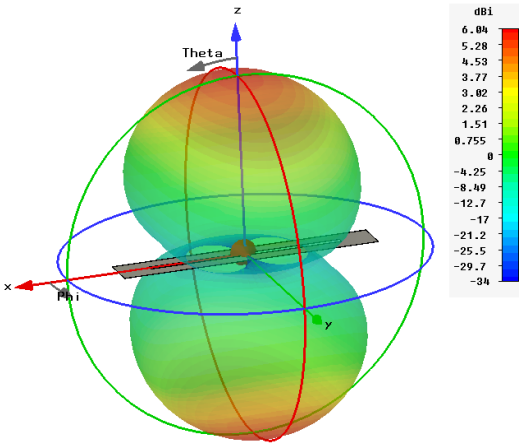

(a) slot antenna

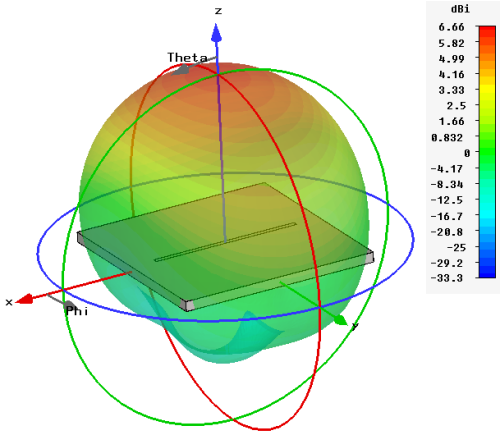

(b) cavity-backed slot antenna

Fig. 3.5 The radiation pattern of a slot and a cavity-backed slot antenna.

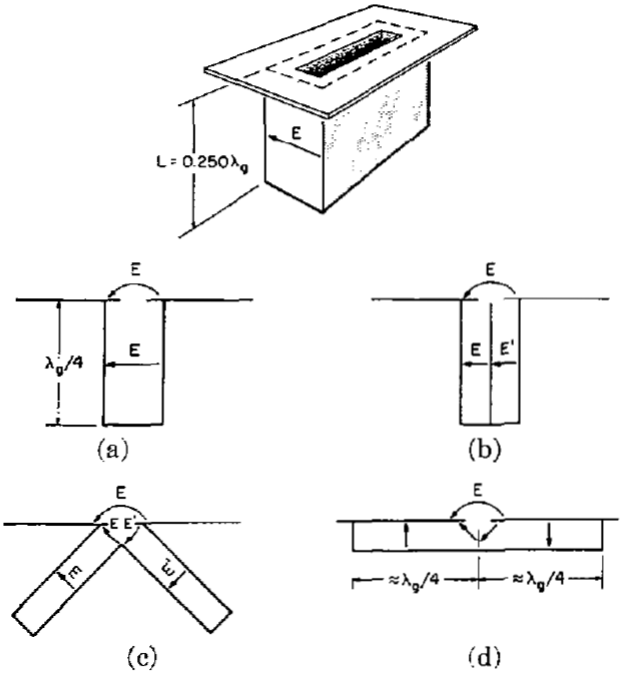

Fig. 3.6 Bending of the cavity-backed slot antenna [31].

3.2.2 Bandwidth and Efficiency Enhancement using Substrate Removal

A technique for enhancement of bandwidth and efficiency of a cavity-backed slot antenna is proposed. The bandwidth of the cavity-backed slot antenna depends on the Q of the slot and the cavity. The proposed technique removes the substrate under the slot to decrease the capacitance of the slot. Because a half-wavelength slot is considered a parallel resonant circuit at resonant frequency, lowered capacitance

increases the bandwidth of the antenna. Antenna efficiency also can be enhanced by the proposed technique. The dielectric loss, which is produced by the E-field across the slot, is effectively decreased by removing the substrate under the slot. Various simulation results of demonstration of the proposed technique are given. The proposed antenna, which was fabricated on a 2 mm height FR-4 substrate, shows 6.2%p higher antenna efficiency and 24% wider bandwidth compared to the conventional cavity-backed slot antenna, which has a whole substrate. The proposed technique is effective in enhancing the efficiency and bandwidth of a cavity-backed slot antenna.

3.2.2.1 Introduction

On the surface of a highly lossy medium, such as a human body, antenna efficiency drops significantly because of dielectric losses in the lossy medium. A cavity-backed slot antenna, which has high radiation efficiency on the surface of the lossy medium, has several attractive features like a planar surface and high productivity. A cavity-backed slot antenna is a strong candidate for Body Area Network (BAN) applications.

In many BAN applications, a low-profile antenna is highly favorable. In the case of a cavity-backed slot antenna, the height of the cavity can be lowered because the guided wavelength is maintained without reference to the height of the

rectangular cavity. However, a low height cavity causes serious drawbacks, such as a narrow bandwidth [32] and low antenna efficiency. As the generated E-field in the low cavity is stronger than that of the high cavity, the dielectric losses and conductor losses generated inside the cavity is larger than those of the high cavity.

Various techniques are suggested to overcome the narrow bandwidth of the cavity-backed slot antenna. Hybrid Substrate Integrated Waveguide (SIW) cavity modes are used to enhance the bandwidth of the SIW cavity-backed slot antenna [33]. In [34], dual slots are used to create dual resonance. By adjusting the length of each slot, two resonance frequencies can be moved to achieve the wide-band characteristic. In [35], a second fictitious resonant frequency is introduced above the first resonant frequency by using the fictitious short circuit [36].

In this section, a technique for the enhancement of the bandwidth and efficiency of the cavity-backed slot antenna is suggested. The proposed technique removes the substrate under the slot to decrease the Q of the slot. The simulation results for three different substrates are suggested to show the effect of the proposed technique. The measured results of the proposed antenna, which was fabricated on the 2 mm height FR-4 substrate, shows 6.2%p higher antenna efficiency and 24% wider bandwidth compared to those of the conventional cavity-backed slot antenna. The proposed technique is a novel method for enhancing the efficiency and bandwidth of a cavity-backed slot antenna.

3.2.2.2 Operation Principles

Fig. 3.7 shows the geometry of a cavity-backed slot antenna. The half-wavelength slot is located at the center of the cavity surface. The bandwidth of the cavity-backed slot antenna depends on the Q of the slot and the cavity. By lowering the Q of the slot, the antenna bandwidth can be increased.

The half-wavelength slot can be expressed by the parallel resonant circuit. The Q of the parallel resonant circuit is well known as

$$Q = \omega_0 RC \tag{3.1}$$

where ω_0 is the resonant frequency and R, C are the resistance and capacitance of resonant circuit, respectively. Hence, the Q of the slot antenna can be lowered by decreasing the capacitance of the slot. By decreasing the Q of the slot, the bandwidth of a cavity-backed slot antenna can be enhanced.

Fig. 3.8 shows the proposed technique for the decreasing capacitance of the slot. In a conventional cavity-backed slot antenna, the space under the slot is filled with a substrate that has a higher relative permittivity than that of air. The proposed technique removes the substrate under the slot to decrease the effective permittivity of the slot. By removing the substrate under the slot, the capacitance of slot can be

lowered, which causes a decrease in slot Q.

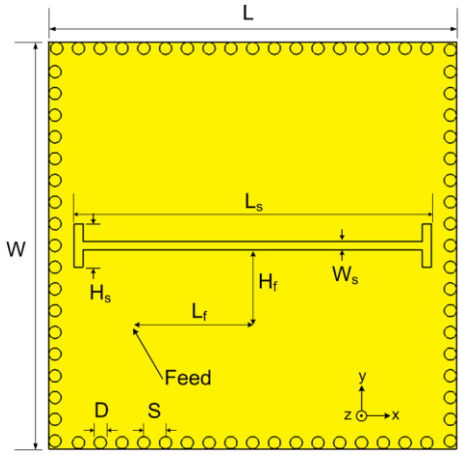

Fig. 3.7 Geometry of simulated and measured cavity-backed slot antenna. (Dimensions of the fabricated antenna, W = 45, L = 55, L_s = 41, H_s = 1, W_s = 1, H_f = 9.5, L_f = 13, D = 0.7, S = 2.5, all in the unit of mm.)

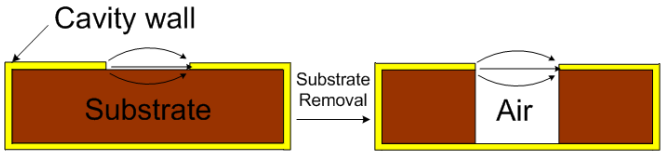

Fig. 3.8 Proposed substrate removal technique for the enhancement of bandwidth and efficiency of a cavity-backed slot antenna.

Lowered capacitance increases the resonance frequency of the resonator. The inductance of the slot should be increased for the compensation of the decreased capacitance. The inductance of the slot can be easily increased by using the longer

TABLE 3.1

DIMENSIONS OF SIMULATED CAVITY-BACKED SLOT ANTENNA. ALL DIMENSIONS ARE IN MILLIMETERS

Substrate	L	W	L_s	W_s	H_s [a]
RT5880	63	55	57	1	4.8
FR-4	45	39	42	1	8.8
RT6010	30	25	28	1	9.6

[a]Dimensions when the height of the substrate is 1 mm, In other substrate heights, H_s is slightly changed for the resonance at 2.45 GHz

slot. However, the compensated longer slot may exceed the size of the cavity, which causes an increase in the size of the antenna.

In the proposed antenna structure, an I-shape slot is used for the inductive loading of the slot. The protruded lengths of each end of the slot determine the increased inductance of the slot [37]. By using the I-shaped slot, decreased capacitance can be compensated without increasing the size of the cavity.

The proposed technique also enhances the efficiency of the cavity-backed slot antenna. In the operation of the slot antenna, an E-field is generated across the slot. However, the E-field, which penetrates the lossy substrate under the slot, causes dielectric losses. This dielectric loss causes a drop in efficiency of the cavity-backed

slot antenna. In the proposed structure, the dielectric losses under the slot decrease considerably because the substrate under the slot is removed. The antenna efficiency is enhanced very effectively on cheap substrates which have high loss tangent. The reduced dielectric loss slightly increases the Q of the resonator. However, this effect on antenna Q can be compensated by the decreased capacitance.

The proposed technique enhances the bandwidth and efficiency of the antenna simultaneously, which are the two main requirements of the antenna.

3.2.2.3 Simulation results

The proposed technique is applied to a conventional cavity-backed slot antenna on three different substrates and compared to conventional cavity-backed slot antennas that have a whole substrate. Duroid 6010 (ε_r = 10.2, tanδ = 0.0023) and FR-4 (ε_r = 4.3, tanδ = 0.015) are selected to observe the effect of the proposed technique in high relative permittivity substrate and lossy substrate, respectively. Duroid 5880 (ε_r = 2.2, tanδ = 0.0009) is selected for the reference substrate. Three different cavity heights (1 mm, 2 mm, 3 mm) are simulated in each substrate. For BAN applications, the antenna is simulated on the body surface, which have a homogeneous electric properties ε_r = 35.15, σ = 1.16 S/m. The distance from the body surface to the cavity bottom is fixed at 0.5 mm.

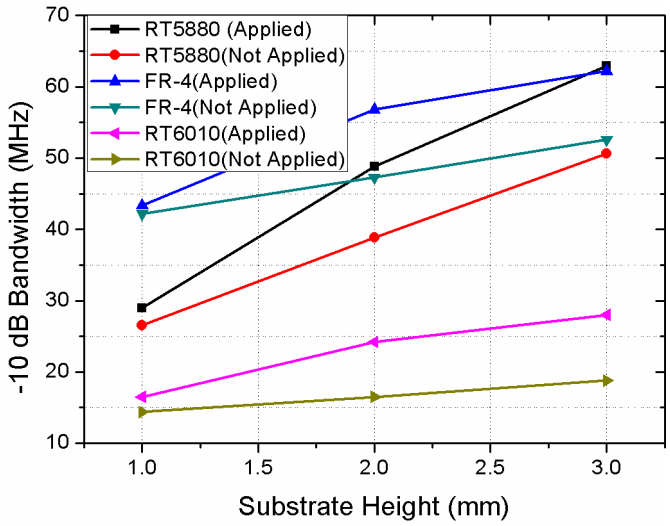

Fig. 3.9 Simulated -10 dB bandwidth of the cavity-backed slot antenna on different substrates.

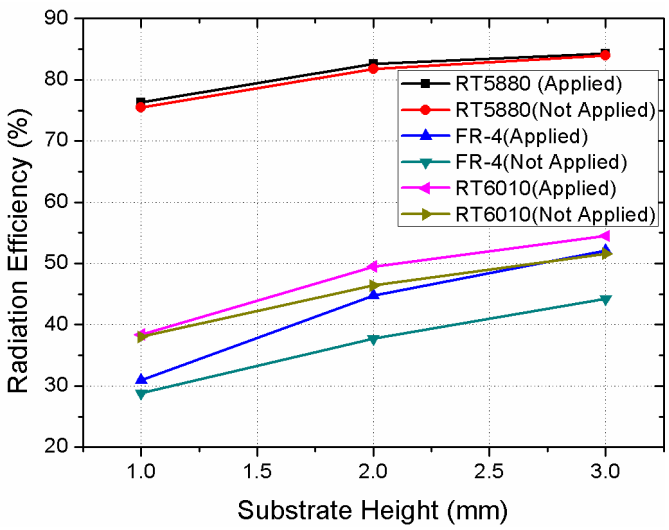

Fig. 3.10 Simulated radiation efficiency of the cavity-backed slot antenna on different substrates.

The length of the slot and the size of the cavity are adjusted to resonate the antenna at 2.45 GHz. Instead of the SIW structure, solid conductor wall cavity is used. The adjusted parameters are described in Table I. Discrete ports are used across the center of the slot to feed the antenna. For simplicity's sake, the port impedance is changed according to the input impedance of the antenna. Because the E-field across the slot is at maximum at the center of the slot and zero at the end of the slot, the input impedance of the antenna can by matched to 50 ohm by moving the location of the feeding point. The simulation is conducted using CST microwave studio.

Fig. 3.9 shows the simulated -10 dB bandwidth of each antenna. As expected, the cavity-backed slot antennas designed with proposed technique have wider bandwidths than those of conventional antennas. Because the Q of the slot is proportional to the relative permittivity of the substrate, the proposed technique is especially useful when the substrate has high relative permittivity. In the case of a cavity-backed slot antenna on the 2 mm height Duroid 6010 substrate, bandwidth that is 46% wider is obtained.

Fig. 3.10 shows the simulated radiation efficiencies of each antenna. The radiation efficiencies of antennas designed with proposed technique are also increased in all substrate. The proposed technique is very effective when the substrate has a higher loss tangent. The cavity-backed slot antenna on the 2 mm

height FR-4 substrate shows a radiation efficiency enhancement of 7.1%p. As the E-field across the slot generates the large dielectric loss in the lossy substrate, the proposed technique is effective on the highly lossy substrate. Because of the low-loss property, radiation efficiencies increased by proposed technique were very small on the Duroid 5880 substrate.

The effect of the removal depth is simulated on the 2 mm height FR-4 substrate. The simulated bandwidth and efficiency are shown in Fig. 3.11. The simulated results show that when the removal depth is deeper than the slot width (1 mm), the effect of the proposed technique is observed sufficiently. The E-field generated across the slot is strong near the slot and weak near the bottom of the cavity. Therefore, the substrate near the bottom of the cavity does not have a strong effect on the operation of the slot. Partially removing the substrate still has the effect of decreasing Q of the slot antenna.

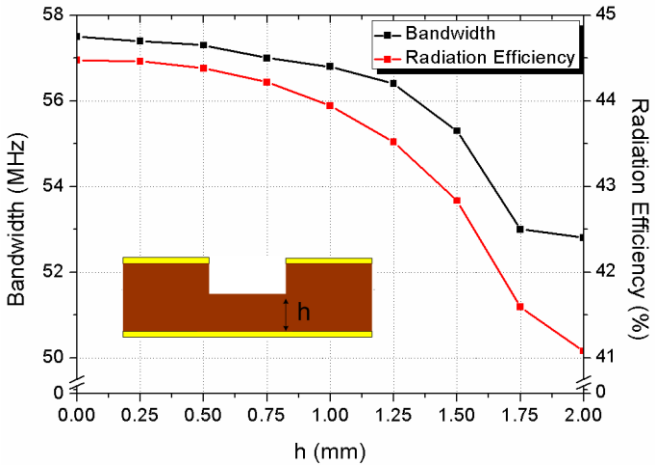

Fig. 3.11 Simulated -10 dB bandwidth with variations of removing depth.

3.2.2.4 Measured Results

The proposed technique can be applied to the any type of cavity-backed slot antennas, cavities of which are filled with substrates. For the demonstration of the proposed technique, cavity-backed slot antenna was fabricated on a 2 mm height FR-4 substrate and compared to the conventional cavity-backed slot antenna, which has a whole substrate. For a fair comparison, equal size cavities were used in both antennas. Slot length was adjusted for the resonance of the antenna at 2.45 GHz. Instead of the solid conductor cavity, a SIW with via conditions (D/S = 0.56, D/λ_0 =0.011) was used to fabricate the antenna using a standard printed circuit board process [38]. At the feeding point, the center pin and the outer conductor of the coaxial cable were connected to the surface and bottom of the cavity, respectively, through the small hole using a SMA connector. The dimensions of the antenna are illustrated on the Fig. 3.7. The fabricated antenna is shown in Fig. 3.12.

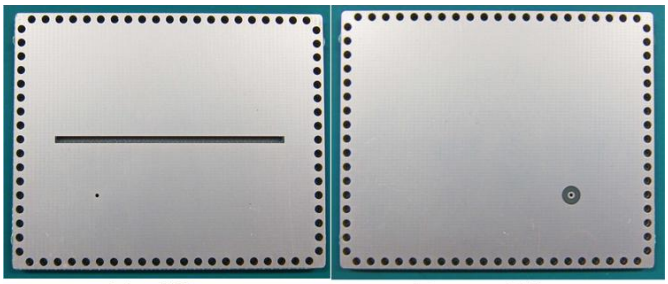

Fig. 3.12 Fabricated Antenna.

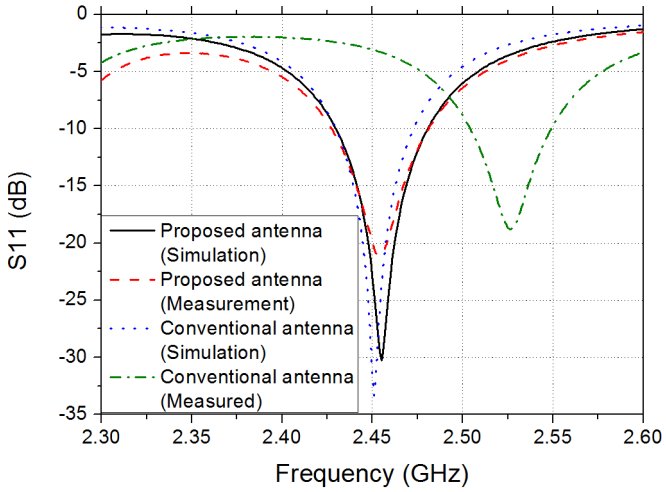

Fig. 3.13. Reflection coefficient of simulated and measured antenna.

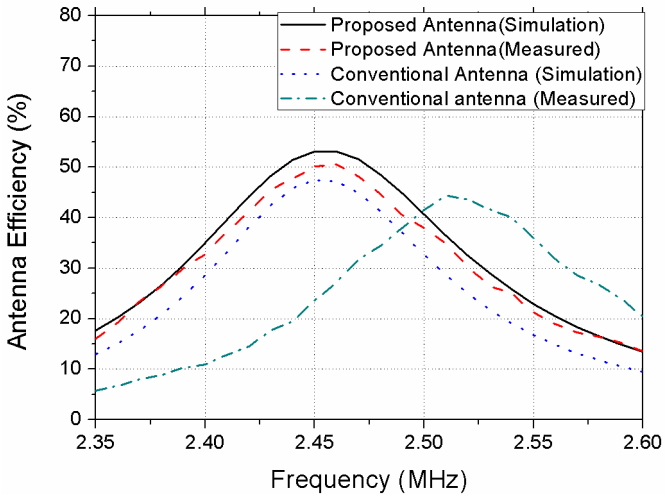

Fig. 3.14. Simulated and measured antenna efficiency.

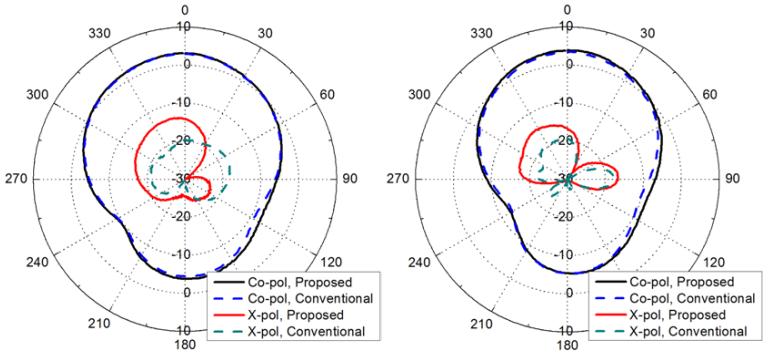

Fig. 3.15. Measured radiation patterns of the proposed and conventional cavity-backed slot antenna (a) E-plane (y-z plane) (b) H-plane (x-z plane).

Fig. 3.13 shows the simulated and measured reflection coefficient of the designed antenna. Although the resonance of the conventional cavity-backed slot antenna is observed at a higher frequency than that of the simulated antenna, similar results were obtained. The difference between the simulated and measured results might have been caused by the electric property variation of the FR-4 substrate. The measured -10 dB fractional bandwidth of the fabricated antenna was 2.16%, which is 24 % wider than that of the conventional antenna.

The Bluetest reverberation system chamber was used to measure the efficiency of the proposed antenna, and the results were compared to the conventional antenna, as shown in Fig. 3.14. The measured antenna efficiency was about 3%p lower than that of the simulated antenna. In the operating frequency, the efficiency of proposed antenna was 50.6%, which is 6.2%p higher than that of the conventional antenna.

The radiation patterns of the fabricated antennas were measured in an anechoic chamber. Fig. 3.15 shows the measured radiation patterns of proposed and conventional cavity-backed slot antenna at 2.45 GHz and 2.52 GHz, respectively. Because of the shifted resonance frequency of the fabricated conventional cavity-backed slot antenna, the radiation patterns of the fabricated conventional antenna are plotted at 2.52 GHz. They are compared in the E-plane (y-z plane) and H-plane (x-z plane). Although the bandwidth and efficiency are enhanced, the radiation patterns of the proposed antenna were similar to those of the conventional cavity-backed slot antenna. Because the proposed technique does not change the symmetric structure of the cavity-backed slot antenna, the radiation patterns of a cavity-backed slot antenna are maintained.

2.2.2.5 Conclusion

A technique for the enhancement of the bandwidth and efficiency of the cavity-backed slot antenna is proposed and demonstrated. The proposed technique can compensate the drawbacks of the high relative permittivity or high loss tangent substrate. The fabricated cavity-backed slot antenna designed using the proposed technique showed 24% wider bandwidth and 6.2%p higher antenna efficiency compared to the conventional cavity-backed slot antenna.

3.2.3 Bandwidth Increase using Via-Hole above the Slot

A novel technique for the bandwidth enhancement of a cavity-backed slot antenna is presented. A via-hole located above the slot creates an additional resonance at a higher frequency by shortening the effective length of the slot. The location of the via-hole can be changed to determine the second resonance frequency of the antenna. With proper placement of the via-hole, the bandwidth of cavity-backed slot antenna can be increased. The fabricated antenna has a 60% wider bandwidth than a cavity-backed slot antenna without via-hole. The proposed antenna maintains high radiation efficiency and gain, which are characteristics of a conventional cavity-backed slot antenna. The proposed technique is especially useful for enhancing the bandwidth of a cavity-backed slot antenna in a limited area.

3.2.3.1 Introduction

In many applications such as Wireless Body Area Network (WBAN) applications, there are strong needs for a low profile antenna. Slot antennas that have attractive features like a planar surface and low profile are very suitable candidates for these applications. On the lossy medium, however, a slot antenna has poor radiation efficiency because of its bidirectional radiation. A cavity-backed slot antenna eliminates the back-side radiation using a quarter wavelength cavity behind the slot. It takes advantage of planar structures and maintains high radiation

efficiency on the lossy mediums.

A quarter-wavelength cavity under the slot may not be suitable in many applications because the cavity increases the height of the antenna. Therefore, a quarter-wavelength cavity is usually bent into the parallel direction with slot to lower the height of the antenna [31]. According to the waveguide theory, the guided wavelength of the rectangular waveguide does not depend on the cavity height. Therefore, the cavity under the slot can maintain its electrical length without reference to the height of the cavity.

However, there are some inherent drawbacks in using a low height substrate in a cavity-backed slot antenna. The height of the substrate affects the Q of the slot and the rectangular cavity. A thin substrate increases the Q of the antenna, which causes a narrow bandwidth [32]. Overcoming a narrow bandwidth is an important issue in designing a low profile cavity-backed slot antenna.

Various techniques have been proposed to overcome the narrow bandwidth of a cavity-backed slot antenna. In [39], two slots are used to create a dual resonance. This technique gives dual-band or wide-band characteristics to the antenna depending on the dimensions of the slots. These antennas show uniform gain over the operating frequency. However, these techniques may increase the size of the cavity to place the two slots on the surface of the cavity. In [40], a varactor-tuned cavity-backed slot antenna with a 1.9:1 tuning range is proposed. At low frequency,

however, the efficiency may be low because of large losses in the varactor.

In this section, a new technique for the bandwidth enhancement of a cavity-backed slot antenna is presented. The proposed antenna only has a via-hole above the slot to create the second resonance. The proposed antenna shows dual resonance without using two slots on the surface of the cavity or special feeding techniques. By adjusting the location of the via-hole, the second resonance can be moved to enhance the bandwidth of main resonance. The fabricated antenna showed uniform gain and antenna efficiency over the operating frequency.

3.2.3.2 Operation Principles

Fig. 3.16 shows the geometry of the proposed antenna. It has a similar geometry to that of a conventional cavity-backed slot antenna except for the single via located above the slot. By using simple rectangular waveguide theory, the dimensions of the cavity are calculated to have a quarter-wavelength in both directions perpendicular to the slot. Instead of the solid conductor cavity, Substrate Integrated Waveguide (SIW) with via conditions (D/S = 0.67, D/λ_0 =0.0065) is used to fabricate the antenna using a standard printed circuit board process [38].

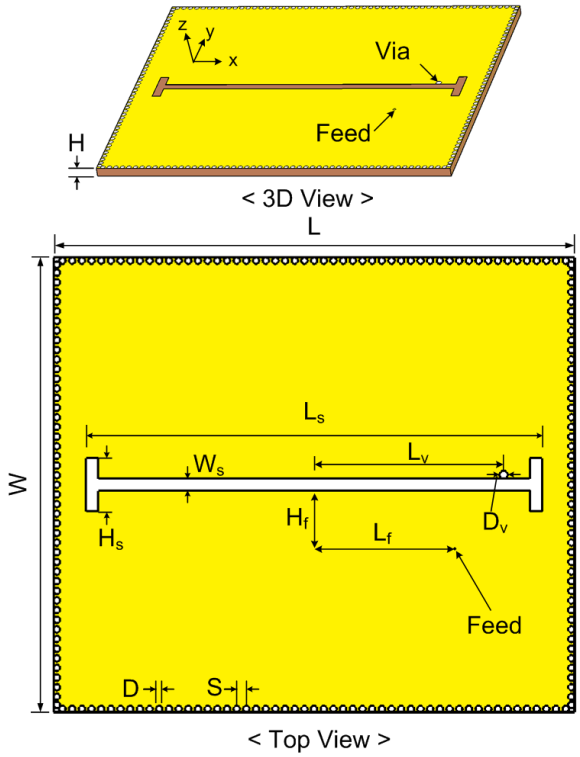

Fig. 3.16. Structure of wide-band cavity-backed slot antenna. (W = 55.8, L = 63.8, H = 1.57, L_s = 55.75, H_s = 6.6, W_s = 1.5, L_v = 23.5, D_v = 1, H_f = 7.25, L_f = 17.5, D = 0.8, S = 1.2, all in the unit of mm.)

The slot is located on the center surface of the cavity. An I-shaped slot is used for an inductive loading of the slot to decrease the slot length. The slot length is approximately a half wavelength at the operating frequency. The via-hole is placed above the slot for the dual resonance. The proposed antenna is fed by a coaxial cable at the bottom of the cavity. At the feeding point, the center pin and outer conductor of the coaxial cable are connected to the surface and bottom of the cavity,

respectively, through the small hole using a SMA connector. The simulation is conducted using CST microwave studio.

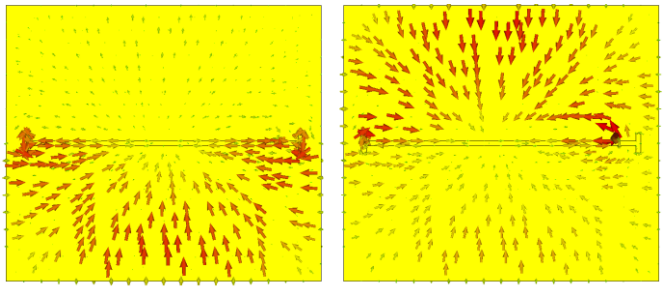

Fig. 3.17. Current distribution of proposed structure at each resonance (a) at first resonance (b) at higher frequency when second resonance occurs.

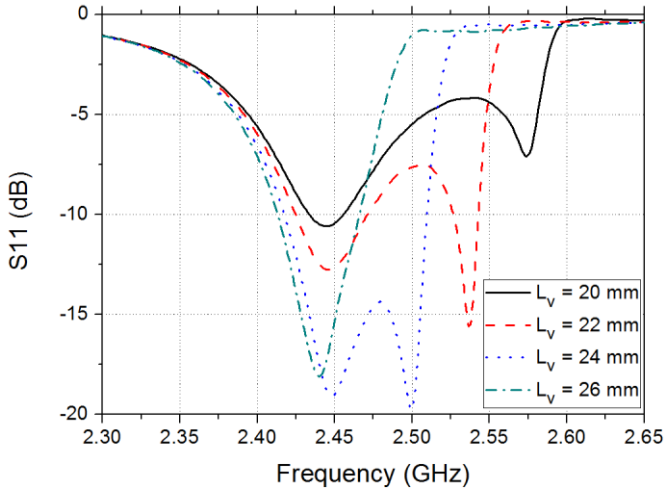

Fig. 3.18. Effect of via location on the reflection coefficient. All other parameters are kept as described in Fig. 3.16

Fig. 3.17 illustrates the current distribution when a normal slot resonance (first resonance) and a higher frequency resonance (second resonance) occur. In a conventional cavity-backed slot antenna, the resonance occurs when the slot has a half wavelength at the operating frequency. The frequency of resonance is mainly determined by the cavity size and the slot length. At first resonance, the minimum current flows to the center of the slot and the maximum current flows to the two edges of the slot in same direction, which is the typical current distribution of a cavity-backed slot antenna.

At second resonance, however, the location where the minimum current flows is slightly moved to the opposite side of the via-hole and maximum current only flows to left edge of the slot. The via-hole, which connects the top surface and the bottom surface of the cavity, creates another route for the current. It shortens the effective length of the slot at a higher resonance frequency.

The second resonance frequency can be changed to a lower or higher frequency by moving the location of the via-hole. Fig. 3.18 shows the simulated input reflection coefficients of the antenna according to the location of the via-hole (L_v). As the via-hole moves to the center of the slot, the second resonance frequency increases. The location of the via-hole does not have a significant effect on the first resonance frequency. By selecting the proper location for the via-hole, wide-band operation can be achieved without significantly changing the first resonance.

A single via-hole is enough to achieve the second resonance; in fact, two via-holes facing each other across the slot may shorten the current flowing to the slot edge. In this case, the first resonance is also affected by the via-hole. Therefore, only a single resonance occurs according to the location of two via-holes.

The proposed structure creates the second resonance without using double slots or special feeding techniques. A single via-hole located above the slot is enough to create a double resonance. This technique is especially useful for enhancing the bandwidth of a cavity-backed slot antenna in a limited area.

3.2.3.3 Measured Results

For the demonstration of the proposed technique, 2.45 GHz was selected as the operating frequency. Cavity size and slot length and width values were determined for the resonance at 2.45 GHz. The parameters H_f, L_f, which relate to the location of the feeding point, were tuned to match the antenna input impedance at 50 ohm. The E-field in Z-direction has a maximum value at the center of the cavity, and decreases as the observation point moves to the edge of the cavity. As a result, the antenna impedance is higher at the center of the cavity and lower at the edge. By moving the feeding location, 50 ohm antenna impedance can be achieved. After determining the antenna geometry, the via-hole location and the diameter are optimized for the maximum bandwidth of the antenna. All optimized antenna parameter values are

described in Fig. 3.16. The designed antenna was fabricated on the substrate with a 1.57 mm height Duroid 5880 that had a relative permittivity of 2.2 and a loss tangent of 0.0009 using a standard printed circuit board process. The fabricated antenna is shown in Fig. 3.19. For measurement, a SMA connector is connected at the bottom of the cavity.

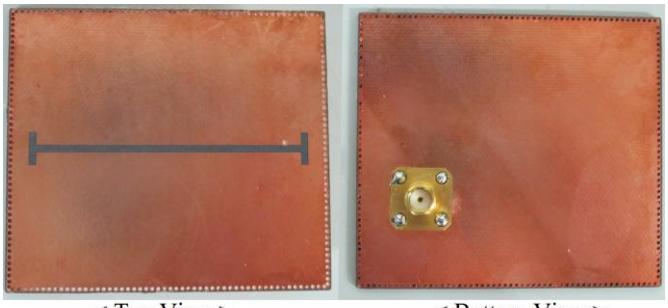

Fig. 3.19. Fabricated wide-band cavity-backed slot antenna.

Fig. 3.20 shows the simulated and measured reflection coefficients of the antenna. Regarding measurement, the -10 dB bandwidth of the proposed antenna is measured to be 82 MHz, which is a similar result to the simulated bandwidth of 91 MHz. The small difference between the two results may have been caused by the fabrication errors in the via-holes. The bandwidth of the proposed structure is very sensitive to the location of the via-hole as displayed in Fig. 3.18.

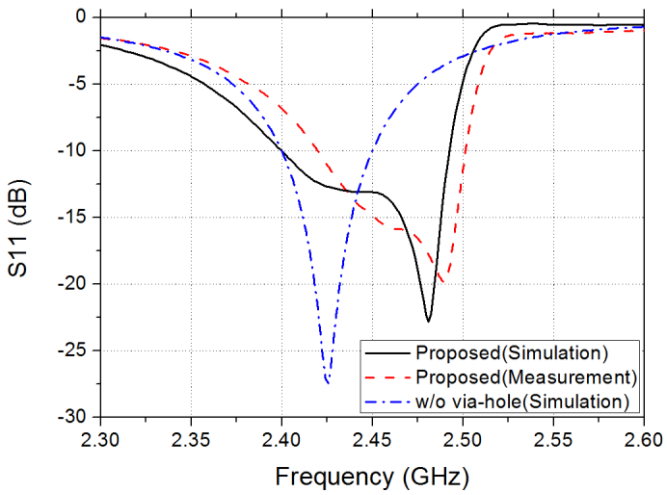

Fig. 3.20. Comparison of the reflection coefficient of the proposed antenna and a conventional cavity-backed slot antenna without via-hole.

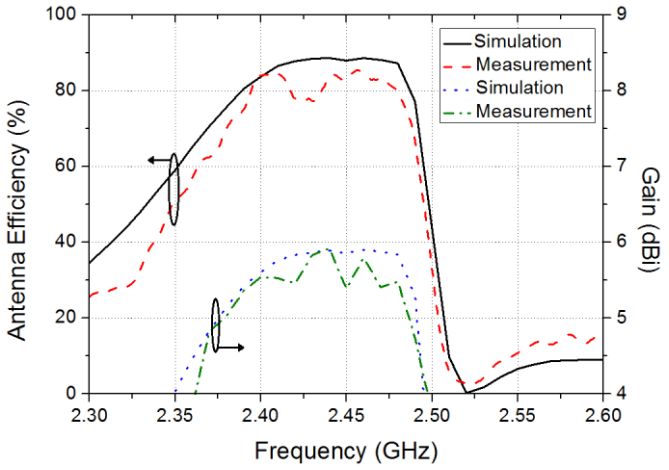

Fig. 3.21. Comparison of measured and simulated total efficiency and antenna gain of the proposed antenna.

In the simulation, a conventional cavity-backed slot antenna with the same dimensions has a 50 MHz -10 dB bandwidth in the given operating frequency. Compared to this result, an approximately 60% wider bandwidth was achieved with the proposed technique.

The antenna efficiency measured in the Bluetest Reverberation Test System chamber is shown in Fig. 3.21. Similar results were obtained with regard to the measured and simulated antenna efficiency. An approximately 80% antenna efficiency was measured in the -10 dB impedance bandwidth. The differences between the two values may have been caused by errors in measurement.

The antenna efficiency drops very rapidly after the second resonance. A quarter wavelength cavity is connected in series with slot antennas in a probe-fed cavity-backed slot antenna. After the dual parallel resonances of the slot, a parallel resonance occurs in the cavity. At the parallel resonance frequency of the cavity, the impedance of the cavity is much higher than that of the slot impedance. Therefore, most energy is consumed in the cavity. This antenna efficiency drop is an inherent characteristic of a coaxial-fed cavity-backed slot antenna.

Measured and simulated antenna gains are also compared in Fig. 3.21. Although the wider-band characteristic, a flat gain higher than 5 dBi is maintained over the -10 dB bandwidth.

The radiation pattern was measured in an anechoic chamber as shown in Fig.

3.22. Measured radiation patterns were compared to simulated radiation patterns in the E-plane (y-z plane) and H-plane (x-z plane) at 2.45 GHz. The radiation patterns of the proposed antenna were very similar to those of a conventional cavity-backed slot antenna. In the boresight direction, the maximum radiation was measured in both cut-planes. The proposed antenna also showed the very low cross-polarization levels in the two cut-planes. In the simulation, cross-polarization in the H-plane was too small to be displayed on the graph. The measured cross-polarization in the H-plane may have been caused by the feeding cable behind the antenna. The front-to-back ratio (FTBR) of the proposed antenna is 12.28 dB at 2.45 GHz. The measured result shows that the proposed antenna keeps its large FTBR.

Although the proposed antenna has a similar gain and radiation patterns to those of a conventional cavity-backed slot antenna, it exhibits a wider-band characteristic that is highly favorable in designing a low-profile cavity-backed antenna.

3.2.3.4 Conclusion

A technique for enhancing the bandwidth of a cavity-backed slot antenna is proposed and demonstrated. By shortening the effective length of the slot at the higher frequency using a single via-hole above the slot, a second resonance is achieved. By moving the second resonance frequency, the bandwidth of a cavity-

backed slot antenna can be increased. Although the fabricated antenna has a 60 % wider bandwidth than a conventional antenna, it maintains the high gain and high antenna efficiency over the -10 dB bandwidth.

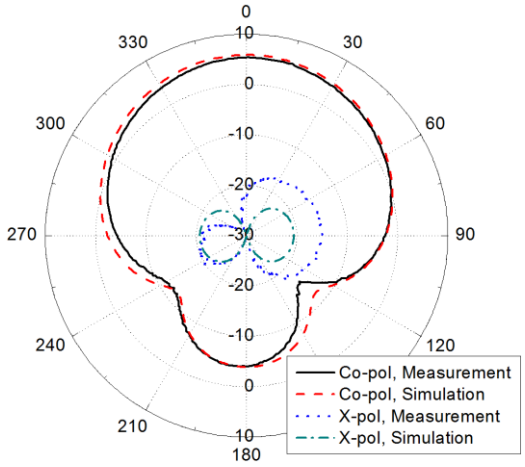

(a) E-Plane

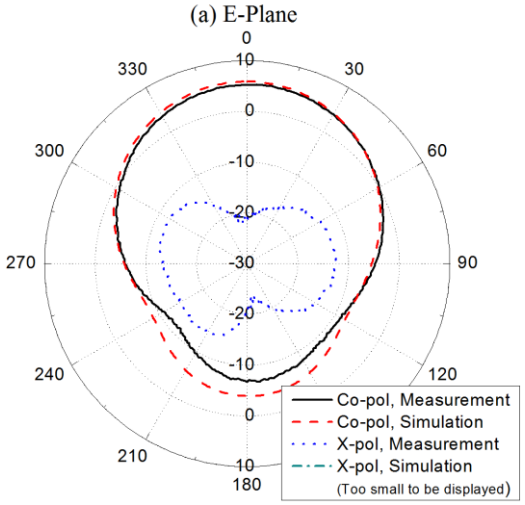

(b) H-Plane

Fig. 3.22 Radiation patterns of the proposed antenna (a) E-plane (y-z plane) (b) H-plane (x-z plane) at 2.45 GHz.

3.2.4 Miniaturization using Folded Cavity Structure

A folded, cavity-backed crossed-slot antenna is proposed for antenna miniaturization. The cavity dimensions of a conventional cavity-backed crossed-slot antenna are about a half guided wavelength along each side, which is unsuitable in many applications like hand-held device or body area network (BAN). To reduce the size of the cavity, a folded cavity is proposed in this section. The center plate that divides the cavity into the upper cavity and the lower cavity increases the effective length inside the cavity. Compared to the conventional cavity-backed crossed-slot antenna, a 72.8% size reduction can be achieved using the proposed structure. The proposed antenna also has circular polarization and wide-band characteristics, which are the main advantage of a cavity-backed crossed-slot antenna. The proposed technique is especially useful for reducing the lateral dimensions of the cavity.

3.2.4.1 Introduction

There is a growing interest in BAN systems that transmit physiological signals to external medical devices. Intensive studies have been conducted on high-efficiency, small BAN application antennas. Unlike antennas in free space, BAN antennas are partly or completely enclosed by the human body depending on their applications. Therefore, it is difficult to design high-efficiency BAN antennas compared to design antennas in free space because of the considerable conductivity

of the human body.

For the high-efficiency on-body antennas, it is desirable for the antenna to have a high front-to-back ratio (FTBR). Compared to the antennas that have an omni-directional radiation patterns, high FTBR antennas are less affected by the material characteristics behind the antenna. A cavity-backed slot antenna is one of the antennas which have high FTBR. A cavity-backed slot antenna eliminates the back radiation from the slot by placing the quarter wavelength cavity behind the slot antenna. As the short-ended quarter guided wavelength cavity has high impedance near the resonance, most of the power radiates through the slot aperture.

In [34], a cavity-backed crossed-slot antenna was proposed for the circular polarization. It has two perpendicular slot pairs on the surface of the cavity. The unequal-length slots cause dual resonance and circular polarization. It has several advantageous characteristics such as wide-band, low-profile, circular polarizations. The circular polarization of a cavity-backed crossed-slot antenna is especially useful in BAN systems where the position and the alignment of antenna can be changed by the movement of the human body. Therefore, the circular polarized antenna is suitable for establishing the reliable channel in the on-body environment. However, the size of the cavity, which is about a half guided wavelength along each side, limits the wide use of a cavity-backed crossed-slot antenna.

Various methods have been proposed for the miniaturization of the cavity-

backed slot antenna. In [41], a specific metallic pattern was used around the slot instead of a solid metal plate. The resonance frequency decreases as the number of strips increases. Decreasing the number of strips causes a radiation efficiency drop because the number of current paths decreases. Negative order resonances are used in [42] to reduce the dimensions of the cavity. As the negative order resonances occur at lower frequency than positive resonance, cavity size reduction can be achieved. The interdigital slots act like a series capacitor and the waveguide's inherent shunt inductor are used for right/left-handed functionality. In [43], miniaturization was achieved by creating a meandering passage from the slot aperture to the cavity wall. This method is useful for reducing lateral dimensions. An H-shaped slot was used to reduce the cavity dimensions [44]. As the H-shaped slot has a longer effective length compared to the straight slot, the overall cavity size can be reduced.

In this section, we propose a folded-cavity structure for the miniaturized cavity-backed crossed-slot antenna. The proposed antenna is similar to the conventional cavity-backed crossed-slot antenna except for folded cavity structure. The center plate, which divides the cavity into two layers, increases the passage length inside the cavity. The measured results showed that a 72.8% size reduction can be achieved with the proposed cavity structure. The performance of the proposed antenna was also measured in on-body environment. The proposed antenna is especially useful in

reducing the lateral dimensions of the cavity.

3.2.4.2 Operation Principles

The length of the conventional cavity is about a half guided wavelength which is determined by the permittivity of the dielectric inside the cavity and lateral cavity length. Therefore, a dielectric with high permittivity is required for the miniaturization of the conventional cavity. However, the use of high permittivity material results in bandwidth and efficiency problems.

To reduce the lateral dimensions, the cavity-backed crossed-slot antenna using folded-cavity is proposed as illustrated in Fig. 3.23. In the proposed cavity structure, the rectangular conducting plate is placed at the middle of the cavity height. The center plate divides the cavity into two layers, the upper layer and lower layer. The two layers of the cavity are connected by the small gap around the center plate. The solid conducting wall enclosing the cavity was replaced by the substrate integrated waveguide (SIW) with via conditions (D/S = 0.56, D/λ_0 =0.0082) for the standard printed circuit board process [38].

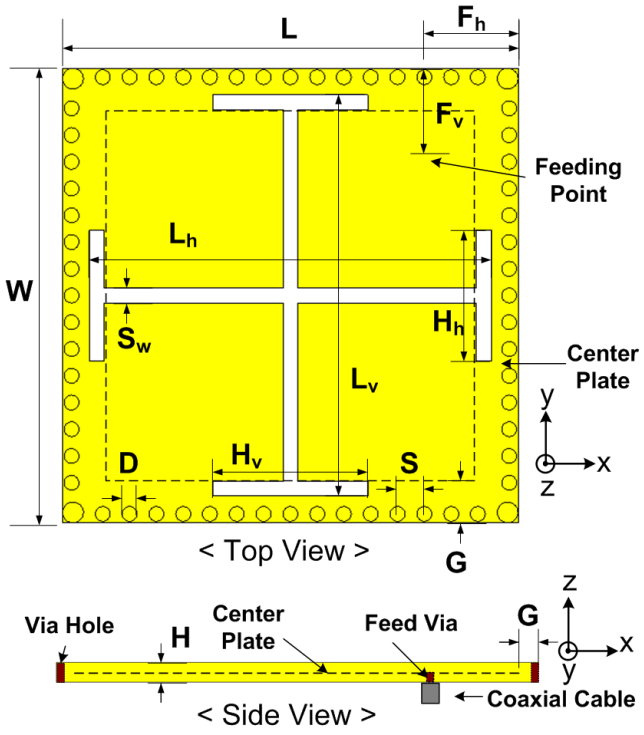

Fig. 3.23. Geometry of the proposed cavity-backed crossed-slot antenna (W = 30, L = 30, S_w = 1, L_h = 27 L_v = 27, F_h = 10.9, F_v = 10.9 H_h = 10, H_v = 9.14, G = 3, H = 3.14, D = 1, S = 1.8 all in the unit of mm.)

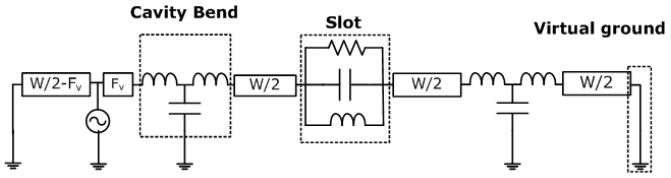

Fig. 3.24. The equivalent circuit of the probe-fed folded cavity-backed slot antenna around the resonance of the slot.

Rogers RT 5880 with a height of 1.57 mm was used for upper and lower layer of cavity, respectively. The total thickness of antenna was 3.14 mm. In the applications where the thickness of antenna is an important issue, we can use thinner substrate because the thickness of a rectangular waveguide does not affect the guided wavelength. However, using thin substrate may degrade the bandwidth and efficiency of the antenna.

The equivalent circuit of probe-fed folded cavity-backed crossed-slot antenna around the resonance of the horizontal slot is plotted in Fig. 3.24. The resonance of the vertical slot occurs orthogonally with the horizontal slot resonance. The half-wavelength slot can be represented by the parallel resonator around the resonance. Considering the accumulation of charge at the bend corner and the current flow interruption, the cavity bend is modeled as series inductors and parallel capacitors. The capacitance in the bend model is determined by the gap dimensions (G) which connect the upper and lower layer of the cavity. As the narrow gap has high capacitance, the narrower gap lowers the resonance frequency. Compared to the conventional cavity, the folded cavity can reduce the lateral dimensions of the cavity by increasing the effective length of the cavity.

The size of the proposed antenna is 30 x 30 x 3.14 mm^3. Compared to the conventional cavity-backed crossed-slot antenna, 72.8% lateral size reduction is achieved. For further size reduction, the solid conducting side wall can be utilized

instead of SIW structures. Using the proposed cavity structure, we can effectively reduce the lateral dimensions of the cavity without using high relative permittivity substrate.

Two slots with different lengths were placed at on the top surface of the proposed cavity. Jerusalem cross-shaped slots were used instead of straight slots for antenna miniaturization. Two slots were placed perpendicular to each other for circular polarizations. To show the resonance characteristics of the proposed antenna, the simulations were conducted using CST Microwave Studio.

Fig. 3.25 shows the simulated reflection coefficient of the antenna and z-directional E-field distributions inside the cavity at each resonance. The resonance frequency of the proposed antenna is strongly affected by the slot length. Two resonances were separated by increasing the length of longer slot as described in Fig. 3.25 for the clear illustration of each resonance mode. As the horizontal slot was longer than the vertical slot, the horizontal slot resonated at a lower frequency than that of the vertical slot.

The E-field distribution at each resonance is quiet similar to that of the conventional cavity-backed slot antenna. In each resonance frequency, odd-mode E-field is generated across the resonating slot. In the conventional cavity-backed slot antenna, it requires the side wall for shorting the quarter wavelength waveguide. In the proposed structure, however, the shorting the waveguide is unnecessary because

the odd mode E-field is generated inside the lower cavity. The virtual ground caused by odd mode E-field serves as shorting wall. The side walls of the cavity operate as the top plate of the conventional cavity.

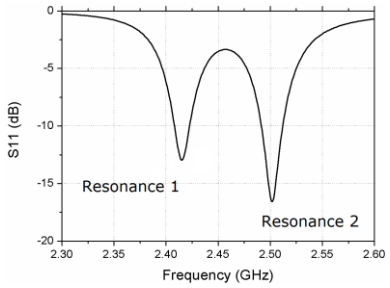

(a) Resonances of the proposed antenna

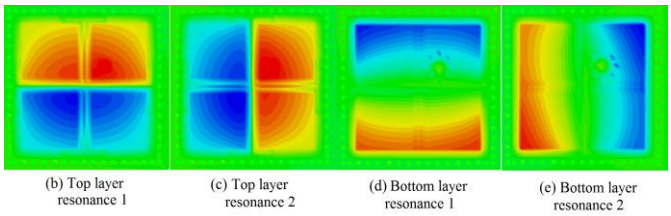

Fig. 3.25. Z-directional E-field distribution inside the proposed antenna cavity at each resonance when H_h = 10, H_v = 8, the other antenna dimensions were kept same as described in Fig. 3.23

At the first resonance where the horizontal slot is excited, the vertically polarized E-field is generated from the horizontal slot. In the same manner, the horizontally polarized E-field is generated from the vertical slot at second resonance. It is possible to generate the circular polarization by using two perpendicular

polarizations. The type of the circular polarization can be controlled by the feeding positions. The proposed antenna primarily generates right-handed circular polarization (RHCP) over operating frequency. The main polarization can be changed to left-handed circular polarization (LHCP) simply by moving the feeding positions across the slot without adjusting the antenna dimensions.

3.2.4.3 Measured Results

A folded cavity-backed crossed-slot antenna was optimized for the circular polarization and fabricated. As the magnitude and the phase of the wave radiated from the each crossed slot determine the axial ratio of the proposed antenna, the lengths of the each slot were determined for low axial ratio. Usually, the antenna design for optimum wide impedance bandwidth is not compatible with optimum circular polarization design. The tradeoff between impedance bandwidth and the axial ratio bandwidth should be considered in the proposed antenna. All optimized antenna dimensions are illustrated in the Fig. 3.23.

For the two-layered structure, the top and the bottom layers were fabricated independently and stacked using screws at each corner. The bottom layer of upper substrate and the top layer of lower substrate were utilized for the center plate.

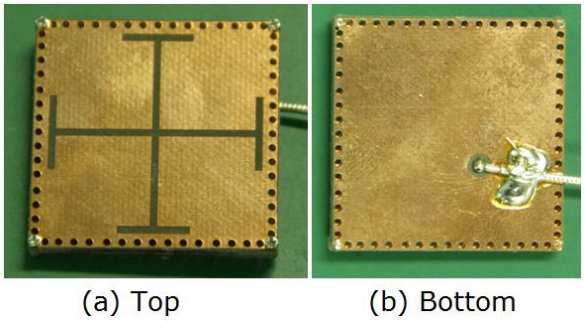

Fig. 3.26. The fabricated antenna

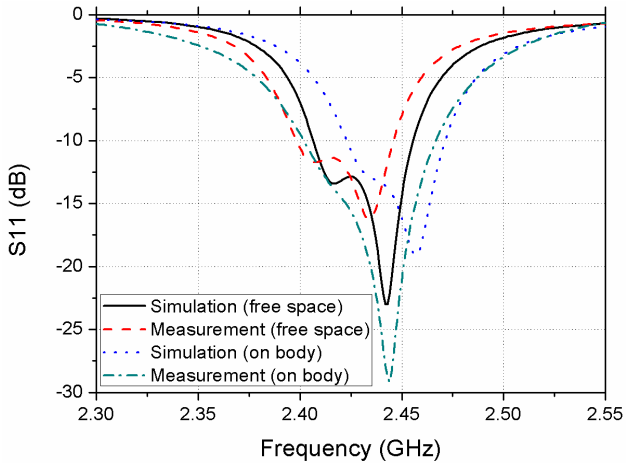

Fig. 3.27. The reflection coefficient (S11) of the measured and simulated antenna.

The optimum feeding position for 50 ohm impedance matching was found by simulation. As illustrated in Fig. 3.25, the E-field magnitude decrease as the feeding point moves from the center of the cavity to the cavity wall. Therefore, the port impedance also decreases as the port moves to the edge of the cavity. Therefore, the

optimum feeding position for 50 ohm port impedance can be found by moving the port position. The proposed antenna is directly fed by coaxial cable. The center conductor and the outer conductor were connected to the center place and bottom plane of the cavity, respectively. The fabricated antenna is shown in Fig. 3.26.

The simulated and the measured reflection coefficient are plotted in Fig. 3.27. The measured -10 dB impedance was 46 MHz, from 2.4 GHz to 2.446 GHz, which is similar to the simulated -10 dB bandwidth 48 MHz. Two resonances representing the horizontal and vertical slot resonance were obvious in the measured results. The center frequency of the fabricated antenna was about 10 MHz lower than the simulated results. As the lengths of two perpendicular slots determine the resonance frequency, etching variation may have caused center frequency shift.

To investigate the performance of the proposed antenna in on body environment, the simulation of the proposed antenna on layered body environment was conducted [27]. The body was modeled as 3-layered structure and the electric characteristics and the thickness are illustrated in Fig. 3.1. All simulated antenna dimensions and materials were identical to those of the free space antenna. The fabricated antenna was placed on the pork loin for the measurement in anechoic chamber. The flexible cable was used for the close attachment between the proposed antenna and the body.

The measured -10 dB impedance bandwidth of the proposed antenna in on-

body environment was 64 MHz, from 2.402 GHz to 2.466 GHz, which is 18 MHz wider than that of the free space results. Because of the lossy characteristics of the body, the impedance bandwidth is increased. Although the body has high relative permittivity and considerable conductivity, there was only a slight change in the resonance frequency. The insensitive characteristic, which is a main advantage of cavity-back slot antenna, is also preserved in the proposed folded cavity structure.

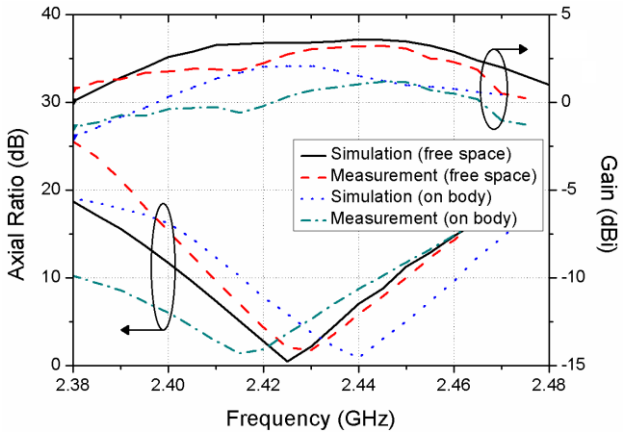

Fig. 3.28. The measured and simulated axial ratio and gain toward the boresight direction.

The radiation patterns and the axial ratio of the fabricated antenna were measured in the anechoic chamber. The measured and simulated boresight direction gain and axial ratio are shown in Fig. 3.28. The measured 3 dB axial ratio bandwidth in free space was 14 MHz, from 2.421 GHz to 2.435 GHz. The on body measurement also showed that the proposed antenna has similar 3 dB axial

bandwidth, from 2.408 GHz to 2.423 GHz, except the frequency shift. The whole 3 dB axial bandwidth is covered by the -10 dB impedance bandwidth in both free space and on body environment.

The material property difference between pork and 3-layered human body model depicted in Fig. 3.1 may have caused the frequency shift. The peak gain of fabricated antenna was measured to be 3.02 dB, which is slightly lower than the simulated peak gain 3.58 dB. The simulated peak gain of proposed antenna in on-body environment was 1.5 dB, which is 2.08 dB lower than that of free space result. Although including the body model had decreased the peak gain, it still maintains considerable gain.

The measured and simulated radiation patterns and axial ratio are plotted in Fig. 3.29 and Fig. 3.30, respectively. The radiation pattern of the proposed antenna is similar to that of the conventional cavity-backed slot antenna. The 3 dB AR beamwidths were measured to 71° (on body), 81° (free space) in the x-z plane. In the y-z plane, 3 dB AR beamwidths were measured to 52° (on body), 133° (free space). The FTBR of the proposed antenna was 4.5 dB, which is a lower value than that of a conventional cavity-backed slot antenna. This is due to the fact that the current flowing along bottom surface is increased by using the folded cavity structure. The FTBR can be enhanced by using a thicker substrate.

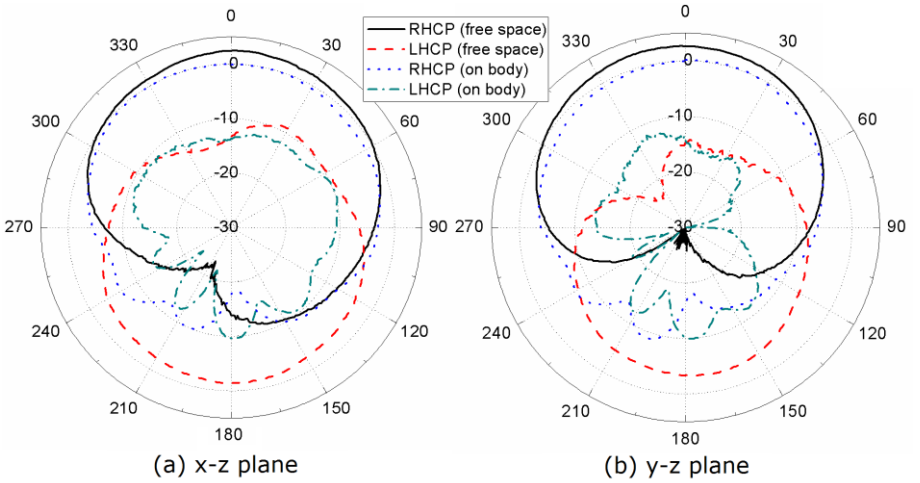

Fig. 3.29. The measured and simulated radiation pattern at 2.44 GHz

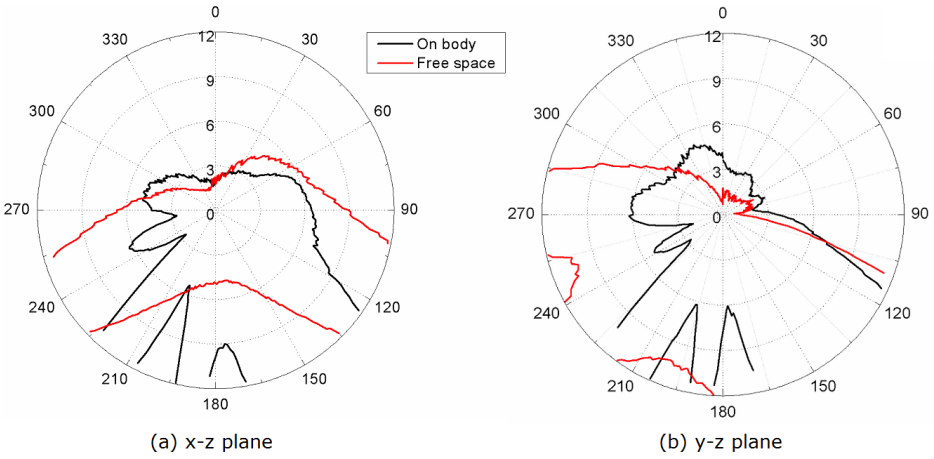

Fig. 3.30. The measured axial ratio of the proposed antenna. The patterns are plotted at 2.42 GHz (on body) and 2.43 GHz (free space).

3.2.4.4 Conclusion

A miniaturization technique for a cavity-backed crossed-slot antenna was proposed and demonstrated. By placing a conducting plate at the middle of the cavity height, 72.8% size reduction was achieved. The proposed antenna also maintains the main characteristics of the cavity-backed crossed-slot antenna like circular polarizations and insensitive characteristics to back side material. The proposed technique is especially useful in reducing the lateral dimensions of the cavity. It is expected to utilizing a cavity-backed crossed-slot antenna in many applications with the proposed cavity structure.

3.2.5 Dual-band Technique for Slot Antennas

A dual-band technique for a cavity-backed crossed-slot antenna is presented. A conventional cavity-backed slot antenna shows the single resonance characteristic which is determined by the lateral length of the cavity and the length of the slot. In this section, dual-band cavity-backed slot antenna is proposed using the series resonator across the slot aperture. As the resonance of the series resonator makes the shorting path across the slot, second resonance can be introduced. The inductance and the capacitance of the series resonator which are implemented by using a straight line and a gap between two lines can be implemented using a standard printed circuit board process. The proposed technique is applied to design the dual-band cavity-backed slot antenna around 2.4 GHz for the demonstration. The simulated antenna showed the dual-band characteristics without increasing the size of the cavity.

3.2.5.1 Introduction

A cavity-backed slot antenna has many advantageous characteristics like planar surface and low profile and high front-to-back ratio (FTBR). The high FTBR of a cavity-backed slot antenna is achieved by using the quarter-wavelength cavity behind slot. This characteristic prevents the cavity-backed slot antenna from the effect of the material behind the cavity. Therefore, a cavity-backed slot antenna is

appealing to the Body Area Network (BAN) where the antenna is backed by the lossy high dielectric constant materials.

One of the main drawbacks of a cavity-backed slot antenna is a narrow bandwidth. Bandwidth of a cavity-backed slot antenna can be enhanced by using thicker cavity or low dielectric constant material. However, these methods increase the dimensions of the cavity. Achieving the dual-band or wide-band characteristic of a cavity-backed slot antenna are comparatively difficult to other antennas like inverted-F antenna because the rectangular cavity structure.

In this section, a dual-band technique for a cavity-backed crossed-slot antenna is presented. The proposed technique makes second resonance by introducing the shorting current path through the series resonator. The inductive and capacitive elements of the series resonator are implemented by using straight line and gap capacitance. The simulated results showed that the dual-band half cavity-backed slot antenna can be designed without increasing the size of the cavity.

3.2.5.2 Operation Principles

The structure of the proposed dual-band half cavity-backed crossed-slot antenna is illustrated in Fig. 3. 31. Because of the symmetric field distribution of the cavity-backed slot antenna, the half cavity is used for antenna miniaturization. The proposed structure is similar to that of a conventional half cavity-backed crossed-slot

antenna except a series resonator across the slot. The series resonator across the slot is connected in parallel with the last part of the slot. In the proposed structure, the straight line and the gap between two lines are used for the implementation of a series resonator. These elements can be simply fabricated with a standard printed circuit board process. By adjusting the length of the line and the gap distance between two lines, the resonance frequency of the series resonator can be controlled.

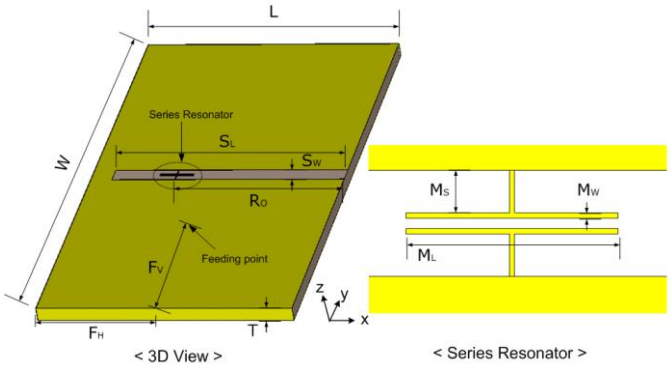

Fig. 3.31. Geometry and dimensions of the proposed dual-band half cavity-backed slot antenna (W = 55, L = 30, S_w = 2, S_L = 27.5, R_O = 20, F_H = 15, F_v = 17.5 M_S = 0.85, M_W = 0.1, M_L = 5, T = 1.57, all in the unit of mm.)

The proposed antenna is fed by a coaxial cable at the bottom of the cavity. The center pin and the outer conductor of the coaxial cable are connected to the top and bottom plate of the cavity, respectively. The feeding position can be adjusted for the 50 ohm antenna impedance. The operating frequency of proposed antenna is set to

2.4 GHz and the series resonator is placed across the slot. The proposed antenna is simulated on the 1.57 mm height Duroid 5880 substrate. All antenna parameter values are described in Fig. 3.31. The simulation is conducted using CST Microwave studio.

3.2.5.3 Simulation Results

The z-directional E-field distribution inside the cavity at each resonance is plotted in Fig. 3.32. Around the first resonance frequency where the slot is about half-wavelength and the series resonator operates as the capacitor, the E-field distribution was similar to that of the conventional cavity-backed slot antenna. The E-field at each side of the slot were opposite direction, exciting the y-directional E-field across the slot. At the second resonance, the impedance of the resonating series resonator was much lower compared to that of the last part of the slot. As a results, the most of the current flows through the series resonator. The effective length of the slot is shortened causing the second resonance at the higher frequency.

The simulated reflection coefficient of the proposed antenna is plotted at Fig. 3. 33. The simulated antenna showed dual-band characteristics. The -10 dB bandwidth were 2.22-2.28 GHz, 3.407 – 3.433 GHz at each resonance. The resonance frequency of first resonance was decreased from 2.4 GHz to 2.25 GHz because of the capacitance of the series resonator. The resonance frequency at each resonance

can be adjusted by changing the structure of the series resonator

The radiation efficiency at 2.25 GHz, and 3.42 GHz was simulated to be 93.6 % and 84.9 %, respectively. The radiation efficiency at the second resonance was lower than first resonance because of the power loss along the series resonator.

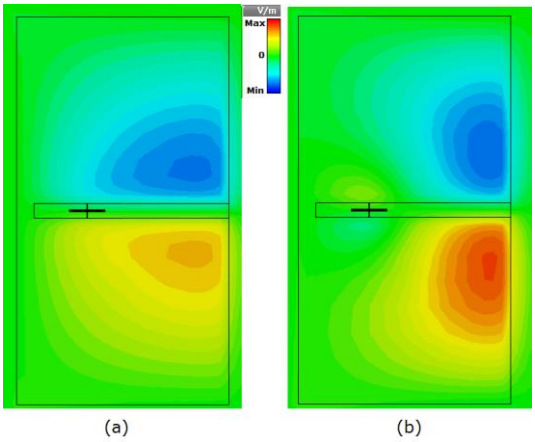

Fig. 3.32. E-field distribution at each resonance (a) 2.25 GHz, (b) 3.45 GHz)

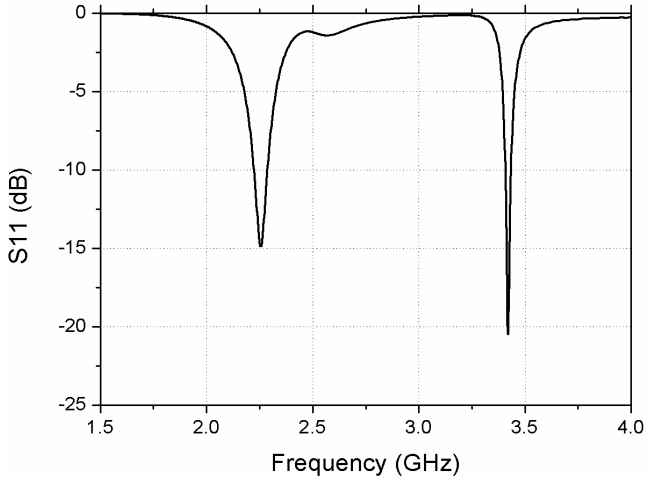

Fig. 3.33. Reflection coefficient of simulated antenna.

3.2.6 Dual Impedance Cavity-backed Slot Antenna

Dual-port cavity-backed slot antenna is proposed for removing a matching circuit between an antenna and a transceiver. The transmitter used in the low power or high power applications has very high or low optimum impedance. Therefore, the matching circuit which has a high impedance transform ratio is needed for impedance matching. The use of a high impedance transform ratio matching circuit, however, may result in narrow band problem or efficiency degradation. For removing the matching circuits, the cavity-backed slot antenna with two different impedance ports is proposed. Each antenna port has an optimum impedance of a transmitter and a receiver. By directly connecting a transmitter and a receiver to the proposed antenna, the matching circuit can be removed from transceiver system. In this section, two port cavity-backed slot antenna which have different input impedance (50 ohm and 100 ohm) is fabricated for demonstration. The measured results show that two ports have a similar bandwidth and radiation patterns. By removing a matching circuit, bandwidth and efficiency of transceiver system can be improved

3.2.6.1 Introduction

In many applications, the optimum impedance of a transmitter is much higher

or lower than 50 ohm. For the case of body area network (BAN) applications, the transmitting power is limited by the safety guide for human body and battery capacity. Consequently, the optimum impedance of the transmitter is much higher than conventional antenna impedance (50 ohm).

In applications where only transmitter is used, various techniques are presented for the impedance matching between an antenna and a transmitter [45-47]. In [45], inductive coupling is used for the impedance matching between dipole antenna and RFID tag chip. The input resistance of antenna can be controlled by the feed loop length. A lumped circuit was used for the impedance matching [46]. Using five discrete lumped components, wideband impedance matching is achieved for short dipole or monopole antenna. Moreover, various impedance techniques are used like T-match, gamma match techniques [47].

However, in transceiver systems where the transmitter and receiver share a single antenna, the antenna impedance cannot be matched to transmitter and receiver simultaneously except transmitter and receiver have same output/input impedance. In this case, the matching circuit should be used between transmitter and receiver independently as depicted in Fig. 3.34. The use of high impedance transform ratio matching circuit may result in narrow band problem. By the effect of finite Q of matching element, power loss also occurs in impedance matching circuits.

In this section, dual-port cavity-backed slot antenna is proposed for removing

matching circuit between an antenna and a transceiver as depicted in Fig. 3.34. Two port antennas usually are used for polarization diversity [39], multi-band [48], and pattern diversity [49]. In this section, we used two-port antenna for impedance matching between antenna and transceiver. The transmitter and the receiver can be directly connected to an each port of the proposed antenna without using matching circuit. Fabricated antenna has dual-port which has different input impedances (50, 100 ohm). The measured results show that each port has a similar bandwidth and radiation patterns, although two ports have different input impedances. With the proposed antenna, input and output matching circuits of a transmitter and a receiver can be removed from the transceiver system. It is expected that systems with proposed antenna have a higher efficiency and wider bandwidth compared to the system with conventional single port antenna and matching circuits.

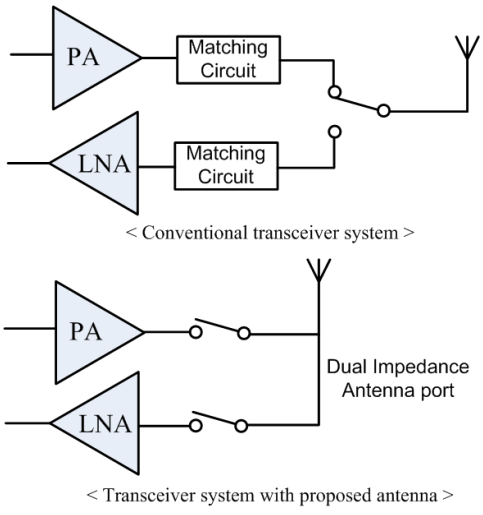

Fig. 3.34. The transceiver system comparison

3.2.6.2 Operation Principles

Fig. 3.35 shows the proposed dual-port cavity-backed slot antenna with different port impedances (50, 100 ohm). The proposed antenna is familiar with conventional cavity-backed slot antenna except the dual-port configuration. Two antenna ports share single slot which is placed at the top surface of cavity.

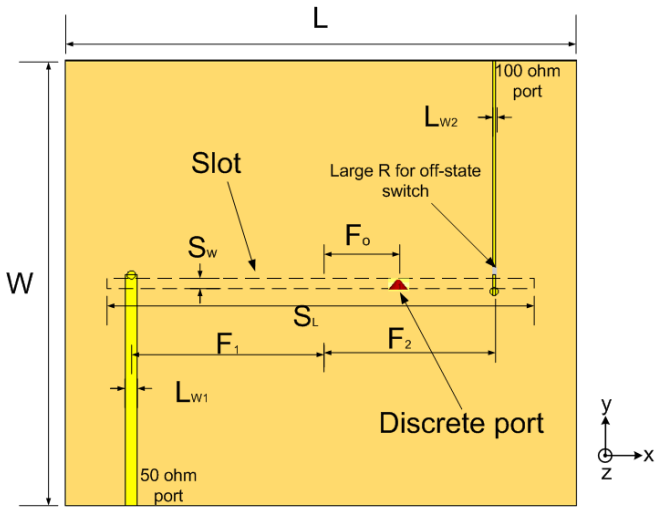

Fig. 3.35 Antenna structure (L = 62, W = 54, S_L = 52, S_W = 1, F_1 = 23, F_2 = 21, L_{W1} = 1.48, L_{W2} = 0.4, all in the unit of mm.)

Two substrates are used for the cavity and microstrip feed, respectively. Instead of the solid conductor cavity, Substrate Integrated Waveguide (SIW) with via conditions (D/S = 0.67, D/λ_0 =0.0065) is used to fabricate the antenna using a standard printed circuit board process [38]. The simulation is conducted using CST microwave studio.

There are various methods for adjusting the input impedance of the antenna. Feeding position control is one of the simplest methods among the proposed methods.

Fig. 3.36 shows the typical E-field (z- direction) distribution of a conventional cavity-backed slot antenna at the first resonance frequency. The magnitude of E-field is largest around the center of the slot and decreases as the observation point moved to the edge of the cavity. As port impedance is proportional to the E-field magnitude at the port, we can control the input impedance of antenna by simply moving the feeding position. The simulated input impedance of cavity-backed slot antenna is plotted in Fig. 3.37 with different feeding positions.

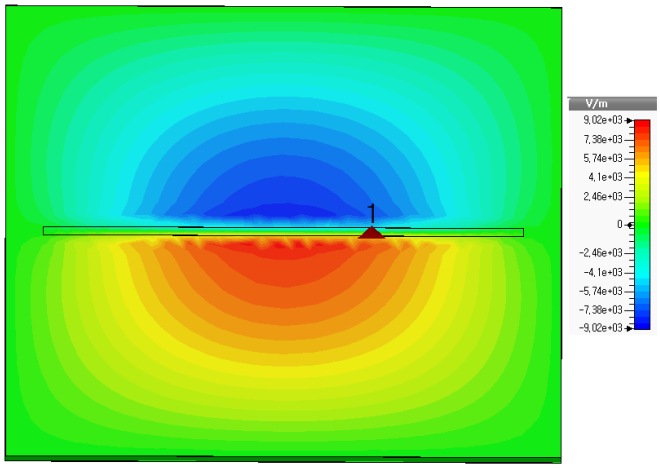

Fig. 3.36. E-field (z-direction) distribution of a cavity-backed slot antenna

As expected from the E-field distribution, the input impedance decreases as the port moves to the edge of the antenna without changing the resonance frequency. The

impedance tuning range depends on the height and electric properties of the substrate. Using RT 5880 substrate of 1.57 mm height, we can control the input impedance up to 600 ohm.

Once the optimum impedances of the transmitter and the receiver are specified, we can find the feeding positions for given input impedance.

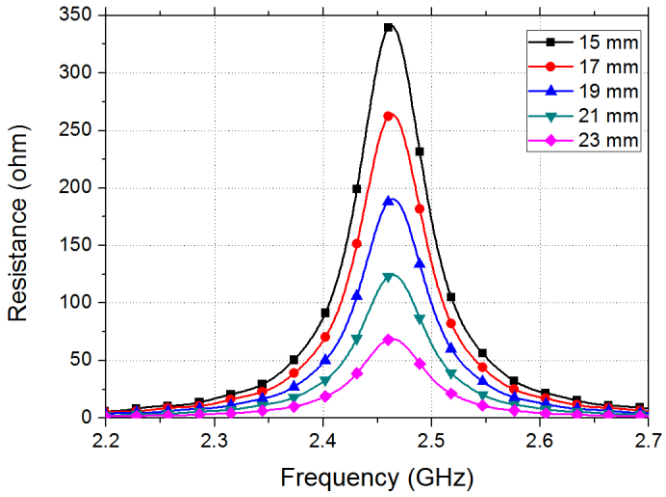

Fig. 3.37. Simulated input resistance with different feeding positions.

Switch is essential component in the systems where the transmitter and receiver share a single antenna. For the switching between transmitting and receiving mode, two single-pole single-throw (SPST) switch or a double-pole single-throw (DPST) switch should be used between a transceiver and an antenna. For the proposed antenna system, two SPST switches are used for switching as illustrated in Fig. 3.34. Two switches change their state depending on the operation of the transmitter and

the receiver. When the transmitter is transmitting, the switch between the transmitter and the antenna changes its state to insertion loss and the other switch changes its state to isolation, and vice versa. Therefore, the antenna can be occupied exclusively by the transmitter or the receiver.

In the system with proposed antenna, it is desirable to two antenna port have similar bandwidth and radiation patterns. However, the feeding line with an isolation switch can affect the operation of an antenna. Since the distance from feeding point and switch has non zero value, the feeding line behaves like open-circuited shunt stub. It adds the shunt capacitance to input impedance of an antenna. Because the equivalent circuit of a slot antenna is parallel resonator around first resonance frequency, adding a shunt capacitance will decrease the resonance frequency of the cavity-backed slot antenna. If the two shunt stub produces same shunt capacitances, the resonance frequencies of each port will identically decrease. However, two same length open-circuit stubs can produce different capacitances because the characteristic impedances of two feeding lines follow the input impedances of their input impedances.

For example, with a dual-port antenna with port impedances 50 and 100 ohm, 50 ohm feeding lines adds more shunt capacitances compared to the same length of 100 ohm feeding line, which results in resonance frequency difference between two antenna ports.

Fig. 3.38 shows the reflection coefficient of 50 ohm antenna port when the switch on the 100 ohm feed line is placed at the different positions from the slot. As expected, the resonance frequency decreases as the distance from the slot to the switch increases.

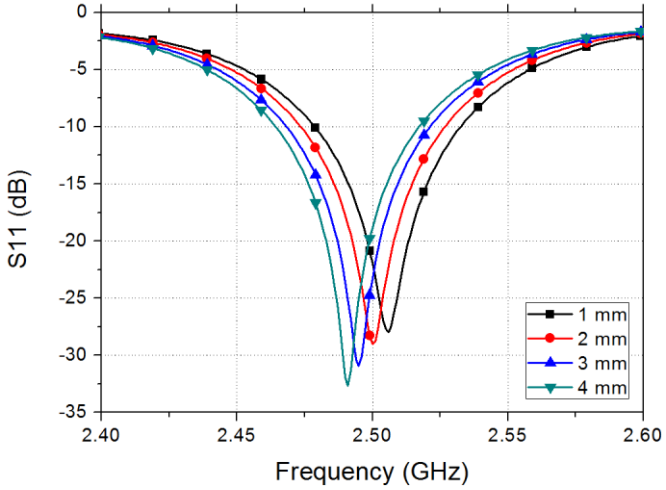

Fig. 3.38. Reflection coefficient of 50 ohm port with different switch position of 100 ohm feeding line.

In the proposed antenna, we placed two switches at the difference distance from the slot. By placing the switch in the low characteristic impedance line closer than the switch in the high characteristic impedance line, the resonance frequency difference can be compensated.

3.2.6.3 Measured Results

For the demonstration of the proposed technique, dual-port cavity-backed slot antenna with input impedances of 50 and 100 ohm was designed and fabricated at

2.5 GHz. RT 5880 which has a relative permittivity of 2.2 and a loss tangent of 0.0009 with a height of 0.5 mm was used for the feed substrate and the cavity substrate. The length of the slot and the cavity were determined for the resonance at 2.5 GHz. After that, feeding positions for 50 and 100 ohm were decided from Fig. 3.37. To feed the antenna at decided feeding positions, two microstrip lines were placed on the top surface of the feeding substrate. The characteristic impedances of the microstrip lines were determined from the target input impedance of each port. Two commercial SPST switches (SKY13347-360LF) which control the operation of each port were located near the slot. The separation distances from the slot to the each switch are determined for the same resonance frequency at each port. Two DC blocking capacitors (47 pF) and biasing circuits were also included for the switch control and the biasing along each feeding line. The fabricated antenna with switch, DC blocking capacitors and biasing circuits are shown in Fig. 3.39.

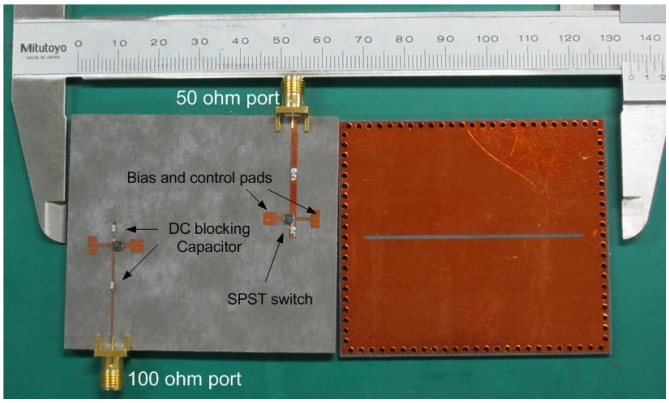

Fig. 3.39. Fabricated antenna

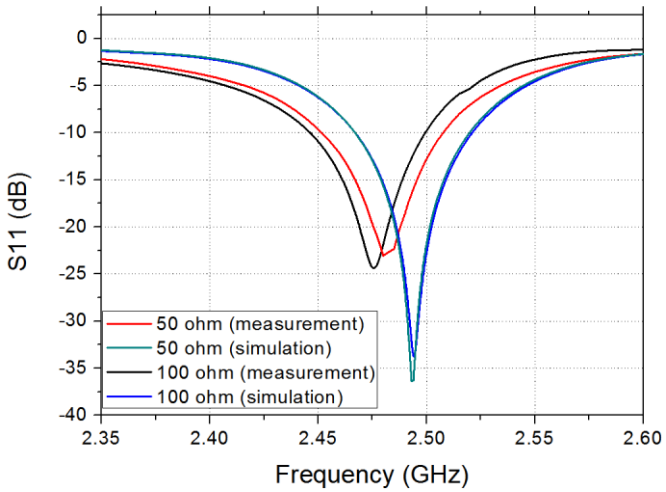

Fig. 3.40. Comparison of the reflection coefficient of 50 and 100 ohm port.

S-parameters were measured using network analyzer (E5071B). The states of two switches are set to isolation or insertion loss depending on the port under measurement. The state of the switch on the 100 ohm feeding line is set to isolation for the measurement of 50 ohm port.

The measured S-parameters are shown in Fig. 3.40. About 14 MHz resonance frequency difference was observed between the simulated and measured results. The parasitic capacitances of the biasing circuits and fabrication errors might cause this difference. Although two ports have different port impedances, the bandwidths were almost same. The -10dB bandwidth of each port was measured to be 55.6 MHz (50 ohm), 55.3 MHz (100 ohm), respectively.

As the isolation between two ports depends on the isolation characteristics of

the applied switch, the isolation is not illustrated in Fig. 3.40. The measured coupling between two ports was less than -20 dB over the all measured frequencies.

The radiation patterns of the each port were measured in the anechoic chamber. As the power supply and wires can affect the radiation patterns of the proposed antenna, a small battery was used for the bias and control of the switch. The negative electrode of the battery is attached to the bottom cavity surface of the proposed antenna. The wires from control and bias pads are connected to positive or negative electrode of battery according to their state.

The measured radiation patterns from 50, 100 ohm port were compared in the E-plane (y-z plane) and H-plane (x-z plane) at 2.48 GHz as shown in Fig. 3.41. Because the two ports share common radiating slot structure, radiation patterns from two slots were similar at both cut-planes. Maximum radiation was observed along the boresight direction. The radiation patterns from two ports were slightly different toward the back side of the antenna. These differences were caused by wires for switch control and battery. In the real system, switches are usually controlled by a switch control unit without the manual wire connections. It is expected that the radiation patterns from both ports will be almost identical without wires and a battery.

The measured results showed that two ports of the proposed antenna have similar bandwidth and radiation patterns, in spite of their different input impedances.

The proposed antenna can be used in the system where the optimum impedances of a transmitter and a receiver are different. Proposed techniques also can be applied to another antenna like dipole and patch antennas by creating the ports in different positions.

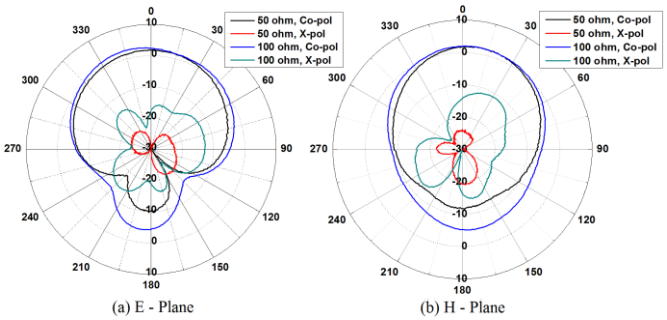

Fig. 3.41. Radiation patterns of the fabricated antenna

3.2.6.4 Conclusion

A technique for removing matching circuit with dual-port cavity-backed slot antenna is proposed. The proposed antenna has dual-port which has different port impedances. As the each port has the optimum impedance of a transmitter and a receiver, a transmitter and a receiver can be directly connected to the antenna without a matching circuit. Two ports with 50, 100 ohm input impedance was fabricated and measured for demonstration. The measured results showed that bandwidth and radiation patterns from two antenna port were similar to each other. The proposed antenna can be used in various systems where transmitter and receiver

have different optimum impedances. Removing matching circuits from the transceiver system with proposed antenna will increase efficiency and bandwidth of the system.

3.3.1 Operation of Shorted Patch Antenna

A patch antenna is widely utilized in various applications like handheld devices, GPS, military, etc. It has many advantages, planar surfaces, low profile, feeding structure, tunability. Similar to the dipole antenna, the overall length of the patch antenna is about half wavelength, which is quiet large in some applications.

Fig. 3.42 shows the E-field distribution when the patch antenna resonates. The anti-symmetric E-field is generated across the center of the patch antenna. The anti-symmetric E-field makes the virtual ground along the center of the patch antenna.

The size miniaturization can be achieved by placing the ground plane along the virtual ground, as shown in Fig. 3.43. Although the size of the patch antenna is decreased to half, the resonance frequency of the patch antenna is maintained. Similar mechanism is applied to the monopole antenna.

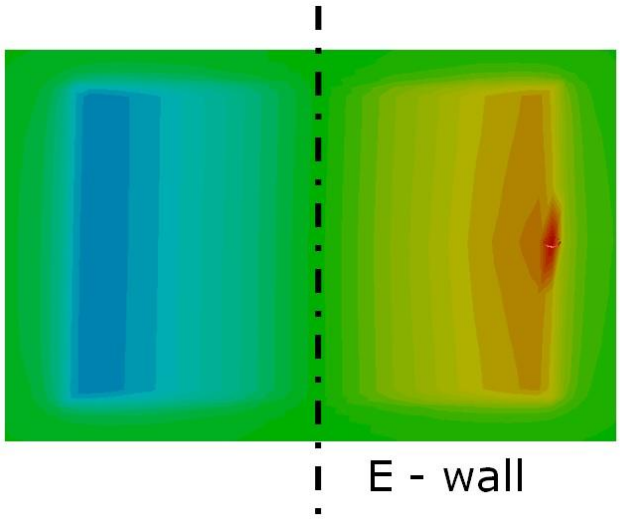

Fig. 3.42. E - field distribution inside the patch antenna

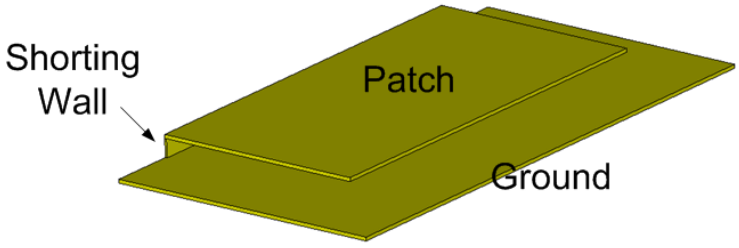

(a) 3D view

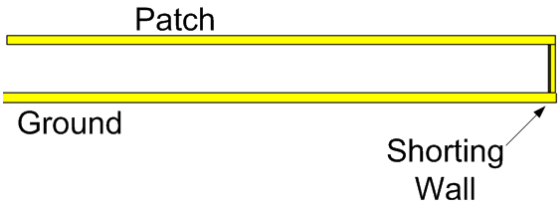

(b) Side view

Fig. 3.43. Shorted patch antenna

3.3.2 Reconfigurable Shorted Patch Antenna

In this section, the reconfigurable shorted patch antenna using switch controls are proposed. The series of via holes which are placed along the side of the shorted patch antenna control the resonance frequency of the patch antenna. By control the switches connected to the via holes, the resonance frequency can be changed. An asymmetric via-hole configuration are utilized for the removal of the overlapping band. The proposed antenna has wide band characteristics from 2.5 GHz to 2.7 GHz.

3.3.2.1 Introduction

Patch antennas that have many attractive features like low-profile, planar surface are widely used in Wireless Body Area Network applications. However, the bandwidth of the patch antenna is relatively narrower than the other antennas. The typical bandwidth of the patch antenna is less the 2 % fractional bandwidth, which may be narrow in some applications.

The reconfigurable antennas are the promising candidates for solving the narrow band problems of the antenna. The resonance frequency of the reconfigurable antenna is controlled by the reconfigurable elements like diode, switch. As the state of the reconfigurable elements affect the operation of the antenna, the resonance frequency can be adjusted. In [50], 4 tuning via holes are placed between the top and the bottom of the cavity-backed slot antenna. The tuning

elements that are connected to the each via hole, controls the resonance frequency of the antenna. In [40], varactor is placed across the slot antenna. The varactor changes the capacitance of the slot antenna, resulting resonance frequency change. The optimum location of the varactor and the feeding line are obtained using the varactor modeling and simulation. The dual patch elements are proposed in [51]. The PIN diodes connecting the each patch element determine the operating patch antenna. As the two patch antennas have different resonance frequency, reconfigurable patch antenna is achieved.

In this sections, the reconfigurable shorted patch antenna is proposed using the via hole control. The proposed antenna has wide bandwidth characteristics from 2.5 GHz to 2.7 GHz.

3.3.2.2 Operation principles

When the shorting wall of the shorted patch antenna covers the entire surface of the patch side, the resonance frequency is maintained identical to that of a full patch antenna. In the case of the shorting wall is shorter than the side length of the patch antenna, the resonance frequency decreases. The length of the shorting wall strongly affects the resonance frequency of the shorted patch antenna. The simulated results

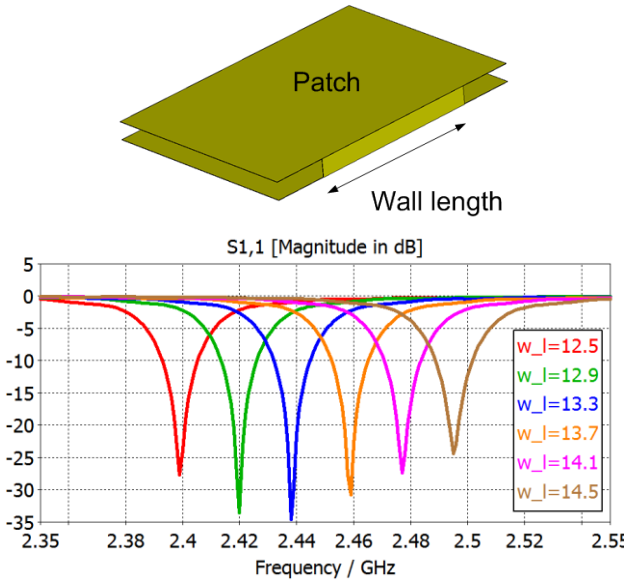

Fig. 3.44. The effect of wall length on reflection coefficient.

shown in Fig. 3.44 shows the effect of the shorting wall length on the resonance frequency of the patch antenna. As the length of the shorting wall decreases, the resonance frequency also decreases. Because the narrow shorting wall increases the inductances, resonance frequency can be changed according to the length of the shorting wall. This is a main operation principle designing the reconfigurable patch antenna.

We placed the 13 via holes between the top and the bottom of the patch antenna, as illustrated in Fig. 3.45. The 10 via holes are fixed and not controlled by the tuning element. The other 3 via holes are controlled by the tuning element. According to the states of the tuning element, the via-hole connections can be controlled. Therefore,

the effective length of the via hole array can be changed by the state of the tuning elements.

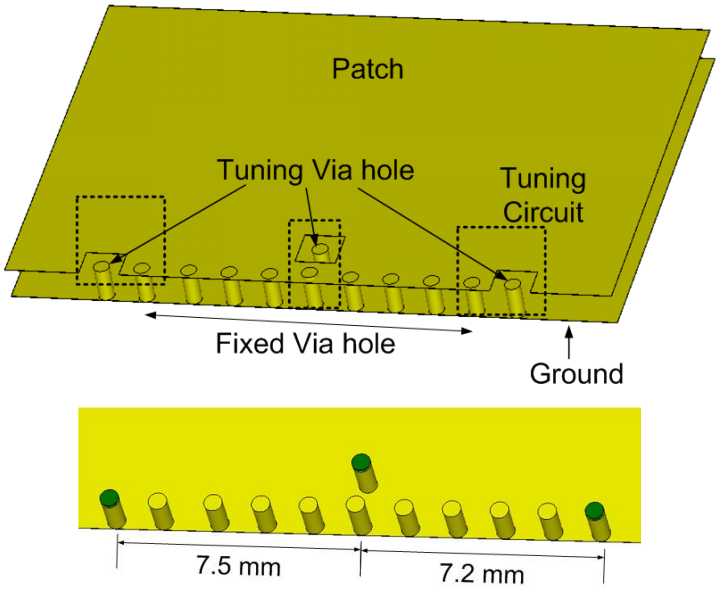

Fig. 3.45. The antenna geometry.

The via-holes placed each ends of the array are not placed symmetrically to remove the overlapping bandwidth. The length of the left via whole array is slightly longer than the length of the right via whole array.

The antennas are fabricated using RT 5880 substrate with a height of 1.57 mm. The upper substrate are added over the top of the patch antenna for the via hole connection control. For the tuning elements, the PIN diode, SMP1320-040LF, is utilized. In the simulation, diode model shown in Fig. 3.46 is considered. The

control circuit shown in Fig. 3.47 is used for the connection control. When the diode is on state, the tuning via holes are connected to the top surface of the patch antenna, increasing the effective length of the via hole array. The simulation was conducted using CST Microwave Studio.

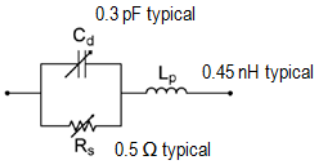

Fig. 3.46. Diode equivalent circuit model.

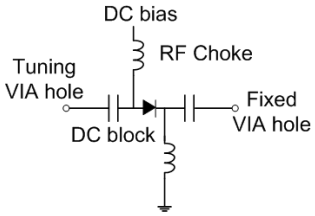

Fig. 3.47. Diode control circuit.

3.3.2.3 Measured results

The fabricated antenna is shown in Fig. 3.48. The DC block capacitors and the RF choke inductors are soldered with diodes. By switching the state of the tuning diodes, the reflection coefficients were measured as shown in Fig. 3.49. The

measured results show that the proposed antenna has a wide -10 dB impedance bandwidth ranging from 2.5 GHz to 2.7 GHz. Considering the fact that the single band shorted patch antenna with a same size has about 50 MHz bandwidth, 4 times bandwidth increase is achieved using the proposed structure. The bandwidth can be further increased by removing the overlapping bandwidth.

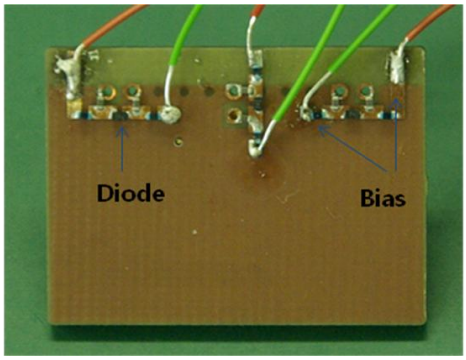

Fig. 3.48. Fabricated antenna

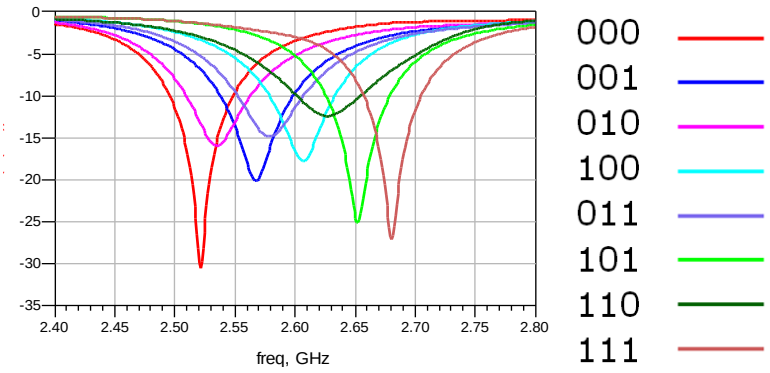

Fig. 3.49. The reflection coefficient at each state. First digit for left switch, middle digit for center diode, last digit for right diode. '0' for off state, '1' for on state.

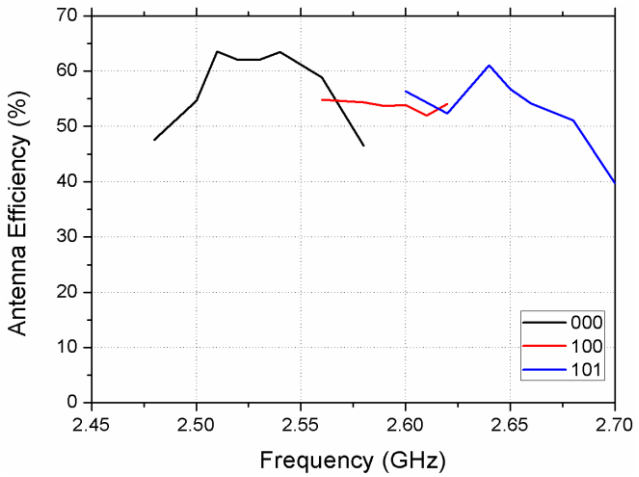

Fig. 3.50. The antenna efficiency of the proposed antenna in 3 states.

The antenna efficiency of the shorted patch antenna is shown in Fig. 3.50 in 3 states. The radiation efficiency was ranged from 50 to 65 %. Compared to the antenna efficiency of a conventional shorted patch antenna, which are ranged from 65 % to 75 %, about 10 % efficiency drop was occurred. The finite Q of the RF choke and the DC block, and the loss in the diodes cause the loss in the reconfigurable shorted patch antenna.

Bibliography

[1] H. Li *et al*., "Trend and standardization of Body Area Network for Medical Healthcare," in *Proc. the 1st European Wireless Technology Conference*, pp.1–4, 2008.

[2] J. Choi *et al*., "A study on the wireless Body Area Network Applications and Channel Models," in *Proc. the 2nd international Conference on Future Generation Communication and Networking*, pp.263–266, 2008.

[3] Y. Hao and R. Foster, "Wireless body sensor networks for health-monitoring applications," *Physiological Measurement*, 29, R27–R56, 2008.

[4] H. S. Nam, H. S. Lee and J. Y. Kim, "Trend of WBAN Application," *Electronic and Telecommunication Trends*, vol. 24, no.5, pp. 109–118, 2009.

[5] L. Stine, "Wireless capsule endoscopy: 'The camera in a pill'," 2005 [Online]. Available: http://www.gihealth.com/newsletter/previous/051.html

[6] W. A. Qureshi, "Current and future applications of the capsule camera," *Nature Rev. Drug Disc*., vol. 3, pp. 447–450, May 2004.

[7] P. M. Izdebski, H. Rajagopalan, and Y. Rahmat-Samii, "Conformal ingestible capsule antenna: A novel Chandelier meandered design," *IEEE Trans. Antennas Propag*., vol. 57, no. 4, pp. 900–909, Apr. 2009.

[8] M. Fonseca, M. Allen, D. Stern, J. White, and J. Kroh, "Implantable wireless sensor for pressure measurement within the heart," U.S. Patent 6855 115, Feb. 15, 2005.

[9] N. Najafi and A. Ludomirsky, "Initial animal studies of a wireless, battery-less, MEMS implant for cardiovascular applications," *Biomed. Microdev*., vol. 6, pp–65, 2004.

[10] R.L. Schneider, N. Najafi, and D.J. Goetzinger, *Anchor for Medical Implant Placement and Method of Manufacture*. Ypsilanti, MI:Integrated Sensing Systems, Inc., 2008.

[11] E. Y. Chow, B. Beier, Y. Ouyang, W.J. Chappell, and P. P. Irazoqui, "High frequency transcutaneous transmission using stents configured as a dipole radiator for cadiovascular implantable devices," presented at the Microw. Theory Tech. Conf., Boston, MA, 2009.

[12] E. Y. Chow, Y. A. L. Chlebowski, S. Chakraborty, W. J. Chappell, and P. P. Irazoqui, "Fully Wireless Implantable Cardiovascular Pressure Monitor Integrated with a Medical Stent," *IEEE Trans. Biomed. Eng*., vol. 57, no. 6, pp.1487 – 1496, June. 2010

[13] Federal Communications commission, "Body Tissue Dielectric Parameters" 2014 [Online]. Available: http://transition.fcc.gov/oet/rfsafety/dielectric.html

[14] R. F. Harrington, "Effect of antenna size on gain, bandwidth, and efficiency," *J. Res. Nat. Bureau Stand*., vol. 64D, pp. 1–12, Jan. 1960.

[15] L. J. Chu, "Physical limitations of omni-directional antenna," *J. Appl. Phys*., vol. 19, pp. 1163–1175, Dec. 1948.

[16] A. Karlsson, "Physical limitations of antennas in a lossy medium," IEEE Trans. Antennas Propagat., vol. 52, no. 8, pp. 2027–2033, Aug. 2004.

[17] Jaechun Lee and Sangwook Nam, "Q Evaluation of Antennas in an Electrically Conductive Medium," IEEE Trans. Antennas Propagat. vol. 56, no. 7, pp. 2116–2120, July. 2008.

[18] Kihyun Kim, Sumin Yun, Sungho Lee, Sangwook Nam, Young Joong Yoon and Changyul Cheon, "A Design of a High-Speed and High-Efficiency Capsule Endoscopy System," *IEEE Trans. Biomed. Eng.* vol. 59, no. 4, pp. 1005–1011, Apr. 2012

[19] G. Iddan, G. Meron, A. Glukhovsky, and P. Swain, “Wireless capsule endoscopy,” *Nature*, vol. 405, no. 6785, pp. 417, May 2000.

[20] K. Kim, M. Jeon, K. Kim, J. Lee, S. Nam, “Human Body Communication Using Chirp Spread Spectrum Modulation,” *The Journal of the Korean Institute of Communication Science*, vol. 35, no. 5, pp. 440–446, May, 2010.

[21] S.I. Kwak, K. Chang, Y.J. Yoon, “Small spiral antenna for wideband capsule endoscope system,” *Electronics Letters*, vol. 42, no. 23, pp. 1328–1329, 2006.

[22] S. H. Lee, Y. J. Yoon, “Fat arm spiral antenna for wideband capsule endoscope systems,” *Radio and Wireless Symposium(RWS)*, pp. 579–582, 2010.

[23] P.M. Izdebski, H. Rajagopalan, Y. Rahmat-Samii, “Conformal Ingestible Capsule Antenna : A Novel Chandelier Meandered Design,” *IEEE Trans. Antennas Propagat.*, vol. 57, no. 4, pp. 900–909, April, 2009.

[24] J. Lee and S. Nam, “Q Evaluation of small Insulated Antennas in a Lossy Medium and Practical Radiation Efficiency Estimation,” *Korea-Japan Microwave conference*, pp.65–68, Nov, 2007.

[25] S. R. Best, “A discussion on electrically small antennas surrounded by lossy dispersive materials,” *Antennas and Propagation, EuCAP 2006*, pp. 1–7, 2006.

[26] K. Kim, S. Lee, E. Cho, J. Choi and S. Nam, “Design of OOK System for Wireless Capsule Endoscopy,” *IEEE ISCAS*, pp.1205–1208, 2010.

[27] A. Christ, A. Klingenbock, T. Samaras, C. Goiceanu and N. Kuster, "The Dependence of Electromagnetic Far-Field Absorption on Body Tissue Composition in the Frequency Range From 300 MHz to 6 GHz," *Microwave Theory and Techniques, IEEE Transactions on*, vol.54, no.5, pp. 2188– 2195, May 2005.

[28] E. Tafeit, R. Möller, K. Sudi, R. Horejsi, A. Berg, and G. Reibnegger, " Orthogonal factor coefficienct development of subcutaneous adipose tissue topography in girls and boys," *Amer. J. Phys. Anthropol*., vol. 115, no. 1, pp. 57–61, Apr. 2001.

[29] T. Abe, D. V. DeHoyos, M. L. Pollok, and L. Garzarella, “Time course for strength and muscle thickness changes following upper and lower body resistance training in men and women," *Eur. J. Appl. Phys*., vol. 81, no. 3, pp. 174–180, Jan. 2000.

[30] D. Phychoudakis, and J. L. Volakis, "Conformal Asymmetric Meandered Flare (AMF) Antenna for Body-Worn Applications," IEEE Antennas Wireless Propag. Lett., vol. 8, pp. 931–934, 2009.

[31] C. A. Lindberg, "A shallow-cavity UHF crossed-slot antenna," *IEEE Trans. Antennas Propag*., vol.17, no.5, pp. 558–563, Sep 1969.

[32] G. Q. Luo, Z. F. Hu, L. X. Dong and L. L. Sun, "Planar Slot Antenna Backed by Substrate Integrated Waveguide Cavity," *IEEE Antennas Wireless Propag. Lett.*, , vol.7, pp.236–239, 2008.

[33] G. Q.Luo, Z. F. Hu, W. J. Li, X. H. Zhang, L. L. Sun and J. F. Zheng, "Bandwidth-Enhanced Low-Profile Cavity-Backed Slot Antenna by Using Hybrid SIW Cavity Modes," *IEEE Trans. Antennas Propag.*, vol.60, no.4, pp.1698–1704, Apr. 2012.

[34] D. Sievenpiper, H. P. Hsu, and R.M. Riley, "Low-profile cavity-backed crossed-slot antenna with a single-probe feed designed for 2.34-GHz satellite radio applications," *IEEE Trans. Antennas Propag.*, vol.52, no.3, pp. 873–879, Mar. 2004.

[35] W. Hong, and K. Sarabandi, "Platform Embedded Slot Antenna Backed by Shielded Parallel Plate Resonator," *IEEE Trans. Antennas Propag.*, vol.58, no.9, pp.2850–2857, Sept. 2010.

[36] N. Behdad, and K. Sarabandi. "A wide-band slot antenna design employing a fictitious short circuit concept," *IEEE Trans. Antennas Propag.*, vol.53, no.1, pp. 475–482, Jan. 2005.

[37] X. Ye, and M. He, "A Compact Circularly Polarized Cavity-Backed Antenna with I-Type Crossed Slot," *Microwave Technology & Computational*

Electromagnetics (ICMTCE), 2011 IEEE International Conference on , pp.31–34, May 2011.

[38] F. Xu, and K. Wu, "Guided-wave and leakage characteristics of substrate integrated waveguide," *IEEE Trans. Microw. Theory Tech.*, vol.53, no.1, pp. 66–73, Jan. 2005.

[39] Y. Liu, Z. Shen, and C. L. Law, "A Compact Dual-Band Cavity-Backed Slot Antenna," *IEEE Antennas Wireless Propag. Lett.*, vol.5, no.1, pp.4–6, Dec. 2006.

[40] C. R. White, and G. M. Rebeiz, "A Shallow Varactor-Tuned Cavity-Backed Slot Antenna With a 1.9:1 Tuning Range," *IEEE Trans. Antennas Propag.*, vol.58, no.3, pp.633–639, March 2010.

[41] W. Hong, N. Behdad, K. Sarabandi, "Size Reduction of Cavity-Backed Slot Antennas," *IEEE Trans. Antennas Propag.*, vol.54, no.5, pp. 1461–1466, May 2006.

[42] Y. Dong, and T. Itoh, ”Miniaturized Substrate Integrated Waveguide Slot Antennas Based on Negative Order Resonance,” *IEEE Trans. Antennas Propag.*, vol. 58, no.12, Dec. 2010.

[43] W. Hong, and K. Sarabandi, "Platform Embedded Slot Antenna Backed by Shielded Parallel Plate Resonator," *IEEE Trans. Antennas Propag.*, vol.58, no.9, pp.2850–2857, Sept. 2010.

[44] W. Xia, K. Saito, M. Takahashi, and K. Ito, “Performances of an Implanted Cavity Slot Antenna Embedded in the Human Arm,” *IEEE Trans. Antennas Propag*., vol. 57, no. 4, Apr. 2009.

[45] H. W. Son and C. S. Pyo, “Design of RFID tag antennas using an inductively coupled feed,” *Electron. Lett.*, vol.41, pp. 994–996, 2005.

[46] V. Iyer, S. N. Makarov, D. D. Harty, F. Nekoogar, and R. Ludwig, A Lumped Circuit for Wideband Impedance Matching of a Non-Resonant, Short Dipole or Monopole Antenna,” *IEEE Trans. Antennas Propag.*, vol.58, no.1, pp.18–26, Jan. 2010.

[47] C. A. Balanis, *Antenna Theory: Analysis and Design*, John Wiley & Sons, New Jersey, 2005, ch. 9.

[48] R. C. Paryani, P. F. Wahid, and N. Behdad, ”A Wideband, Dual-Polarized, Substrate-Integrated Cavity-Backed Slot Antenna,” *IEEE Antennas Wireless Propag. Lett.*, vol.9, pp.645–648, Dec. 2010.

[49] S. S. Yang, and K, Luk, ”Design of a Wide-Band L-Probe Patch Antenna for Pattern Reconfiguration or Diversity Applications,” *IEEE Trans. Antennas Propag.*, vol.54, no.2, pp.433-438, Feb. 2006.

[50] A. P. Saghati, and K. Entesari, "A Reconfigurable SIW Cavity-Backed Slot Antenna With One Octave Tuning Range," *IEEE Trans. Antennas Propag.*, vol. 61, no. 8, pp.3837- 3945,Aug. 2013.

[51] H. F. Abutarboush, R. Nilavalan, S. W. Cheung, K. M. Nasr, T. Peter, D. Budimir, and H. Al-Raweshidy, "A Reconfigurable Wideband and Multiband Antenna Using Dual-Patch Elements for Compact Wireless Devices," *IEEE Trans. Antennas Propag.*, vol. 60, no. 1, pp.36-43, Jan. 2012.

초록

본 논문에서는 인체통신을 위한 안테나의 문제점을 분석하고 이를 해결하기 위한 여러 가지 안테나 구조를 제안하였다. 인체통신용 안테나는 높은 유전율과 도전율을 가지는 인체의 전기적 특성으로 인해 공기중의 안테나에 비해 효율과 대역폭이 크게 감소하게 된다. 하지만 인체통신용 안테나로 사용하기 위해서는 안테나의 소형화가 이루어져야 하기 때문에 소형 크기를 유지하면서 효율과 대역폭을 증가시키기 위한 안테나 구조가 필수적이다. 인체통신용 안테나의 성능을 개선하기 위해서 본 논문에서는 몇 가지 방법이 소개된다.

첫 번째로, 인체 내부에서 동작하는 안테나의 성능을 개선하기 위해 인체 내부에서의 안테나 Q와 효율에 대한 분석을 진행했다. 계산을 통해 주어진 크기에 따른 인체 내부에서 통신을 하기 위한 최적 주파수가 제안되었다. 또한 안테나의 크기를 증가시켜서 성능을 계선하기 위해, 외벽 구조를 최대한 활용한 캡슐 내시경용 외벽 루프 안테나가 제안되고, 다른 안테나의 성능 비교를 통한 측정결과를 보였다.

두 번째로, 인체 위에서 동작하는 인체통신용 시스템을 위한 안테나가 제안되었다. 시뮬레이션을 통해 인체 위에서 상대적으로 높은 효율을 갖는 cavity-backed 슬롯 안테나와 패치 안테나를 중심으로 성능 개선을

위한 구조를 제안하였다. 슬롯 상부의 비아홀을 통한 이중 공진 구조, 기판 제거를 통한 대역폭 및 효율 향상 기술, 또한 안테나 소형화를 위한 접는 cavity 구조 등이 실험결과와 함께 분석되었다. 또한 인체통신용 시스템 효율 향상을 위한 이중 임피던스를 갖는 안테나 구조, 재구성이 가능한 shorted 패치 안테나 등이 제안되었고 실험을 통해 동작을 확인하였다.

주요어: 캡슐 내시경 안테나, cavity-backed 슬롯 안테나, 패치 안테나, 재구성이 가능한 안테나, 광대역, 고효율 안테나, 소형화, 이중대역, 이중 임피던스

학번 : 2008-22942